Supporting Information

# A porous Anderson-type polyoxometalate-based metal-organic framework as multi-functional platform for selective oxidative coupling with amines

Hong-Ru Tan,[a] Xiang Zhou,[b] Hanqi You,[a] Qi Zheng,[b] Sheng-Yin Zhao,[*a] Weimin Xuan[*a]

[a] State Key Laboratory for Modification of Chemical Fibers and Polymer Materials & College of Chemistry and Chemical Engineering, Donghua University, Shanghai 201620, P. R. China. E-mail: syzhao8@dhu.edu.cn, weiminxuan@dhu.edu.cn

[b] State Key Laboratory for Modification of Chemical Fibers and Polymer Materials & College of Materials Science and Engineering, Donghua University, Shanghai 201620, P. R. China. E-mail: qi.zheng@dhu.edu.cn

**Table of contents:**

## 1. General information

### Materials

Unless otherwise noted, all the materials were purchased from commercial suppliers and used without further purification. Petroleum ether (PE) refers to a hydrocarbon mixture with a boiling range of 60-90 ℃.

### Instruments and measurements

NMR ($^{1}H$ and $^{13}C$) spectra were recorded using a Bruker AV 400 & 600 MHz spectrometer in DMSO-$d_6$ and $CDCl_3$ with TMS as internal standard. Chemical shifts (δ) were recorded in ppm.

SCXRD (Single crystal X-ray diffraction): Crystal was coated with Paratone Oil on a Cryloop pin were mounted on a Bruker D8 VENTURE Apex IV single-crystal x-ray diffractometer equipped with a CCD area detector at 1500 W power (50 kV, 30 mA) to generate Mo Kα radiation (λ = 0.71073 Å). The structure was solved by direct methods with SHELXS-2014 and refined with SHELXL-2014 using OLEX 2.13.[1] All the non-hydrogen atoms except guest molecules were refined by full-matrix least-squares techniques with anisotropic displacement parameters. Contributions to scattering due to these highly disordered solvent molecules were removed using the SQUEEZE routine of PLATON; structures were then refined again using the data generated.[2] Crystallographic data for the structures reported in this paper have been deposited in the Cambridge Crystallographic Data Center with CCDC number of 2285696.

Powder X-ray diffraction (PXRD) measurements were performed on a Rigaku D/Max-2550 PC (Japan) diffractometer, using Cu-Kα radiation (λ = 1.541 Å) at 40 kV, 30 mA over the angular range 2$\theta$ 3°–50° at a scan rate of 2° $min^{-1}$.

IR spectra ATR-FTIR spectra were taken on a Nicolet iS□□
(Thermo Fisher Scientific) spectrometer with a diamond ATR crystal as
the window material.

ATR-FTIR spectra were taken on a Nicolet iS□□ (Thermo Fisher Scientific) spectrometer with a diamond ATR crystal as the window material.
ATR-FTIR spectra were taken on a Nicolet iS□□ (Thermo Fisher Scientific) spectrometer with a diamond ATR crystal as the window material.
ATR-FTIR spectra were taken on a Nicolet iS□□ (Thermo Fisher Scientific) spectrometer with a diamond ATR crystal as the window material.

ATR-FTIR spectra were taken on a Nicolet iS50 (Thermo Fisher Scientific) spectrometer with a diamond ATR crystal as the window material in 400-4000$cm^{-1}$.

Thermogravimetric analysis (TGA) was conducted under a nitrogen atmosphere with a heating rate of 10 °C $min^{-1}$ on a TG 209 F1 Libra® up to 800 °C.

The $N_2$ adsorption isotherms were collected at 77 K on an Autosorb-iQ/Autosorb-iQ instrument with micropore option used.

TLC was performed on silica gel polygram SILG/UV 254 plates and visualized by quenching of UV fluorescence ($\lambda_{max}$ = 254 nm). Silica gel (100-200 microns) was used

for all chromatographic separations.

GC-MS analysis was carried out on an Agilent 8860 GC system and 5977B GC/MSD system with EI mode.

Elemental analysis (C, H and N) was performed on a VarioEL III elemental analyzer. Y, Cr and Mo were analyzed using a Prodigy-ICP atomic emission spectrometer.

## 2. Experimental procedures

1,1'-bis(4-carboxybenzyl)-[4,4'-bipyridine]-1,1'-diium dichloride ($H_2$**L**$Cl_2$) was synthesized according to the literature.[3] 5g 4,4'-bipyridine (32mmol) and 12g 4-chlorine methyl benzoic acid (70.4 mmol) was added into 50 mL DMF, the mixture was reflux for 8 h. The resulting precipitate was obtained and washed by DMF, EtOH and $Et_2O$. The white solid was dried at 80 ºC. Yield: 15.5g (97.3%). $^1$H NMR (400 MHz, DMSO-$d_6$) δ 9.64 (d, $J$ = 6.2 Hz, 2H), 8.84 (d, $J$ = 6.2 Hz, 2H), 8.01 (d, $J$ = 7.9 Hz, 2H), 7.75 (d, $J$ = 7.9 Hz, 2H), 6.12 (s, 2H).

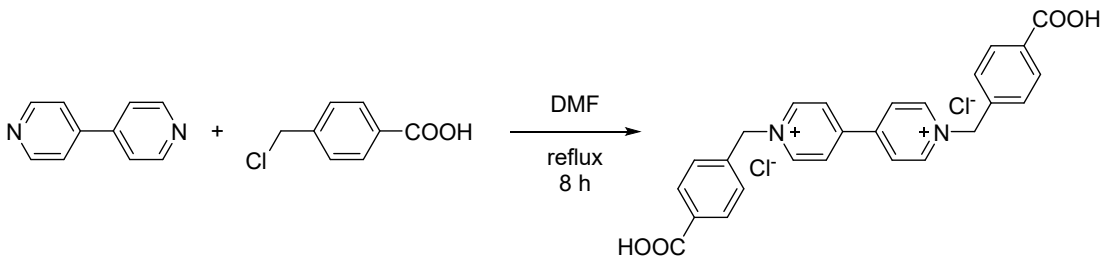


$Na_3[Cr(OH)_6Mo_6O_{18}]$ (CrMo6) was synthesized according to the literature method.[4] The pH of a solution containing 145 g $Na_2MoO_4{\cdot}2H_2O$ (0.6 mol) in 300 mL of water was adjusted to 4.5 with concentrated $HNO_3$. A second solution was made by dissolving 40.0 g $Cr(NO_3)_3{\cdot}9H_2O$ (0.1 mol) in 40 mL water. Half of each solution was mixed together, and the mixture was boiled for 1 min and filtered while hot. The filtrate was set aside in a 1500 mL beaker for 2 weeks before the precipitate was filtered off and washed several times with cold water. The pink crystal was dried in the air. Yield: 38.5 g (32.2% based on Cr). FI-IR ($cm^{-1}$): 3460, 3125, 1647, 1617, 963, 927, 886, 814, 740, 630.

$[(C_4H_9)_4N]_3CrMo_6O_{18}[(OCH_2)_3CCH_2OH]_2{\cdot}2DMF$ (**CrMo6-PET2**) was synthesized according to the literature.[5] 2.18 g $Na_3[Cr(OH)_6Mo_6O_{18}]$ (2 mmol) and 0.81 g pentaerythritol (6 mmol) were dissolved in 60 mL deionized water to form a clear purple solution and the resulting solution was sealed in a 100 mL stainless steel reactor with a Teflon liner and heated at 140 ºC for 24 h. After cooled down to room temperature, 2.0 g TBA-Br (tetrabutylammonium bromide) was added into the solution and light purple precipitation began to form immediately. The precipitation was filtered off and dried in the air. The crystals could be obtained by ether diffusion into DMF for 2 days. Yield: 2.5 g (65.8% based on Mo). FI-IR ($cm^{-1}$): 2958, 2871, 1656, 1474, 1379, 1117, 1023, 909, 641.

Synthesis of **POMOF-1** ($Y\mathbf{L}_2(H_2O)_2[CrMo_6O_{18}(PET)_2]\cdot 4H_2O$). 1.53 mg (0.004 mmol) $Y(NO_3)_3\cdot 6H_2O$, 2.29 mg (0.0046 mmol) **L** and 7.66 mg (0.0046 mmol) CrMo6-PET2 were added into 0.5 mL DMA and 0.5 mL $H_2O$. The mixture was heat at 80 ºC for 12 h and the pink bulk crystal was obtained after cooling to room temperature. (Yield: 4.2 mg. 38.2 % based on Y). Elemental analysis for **POMOF-1**: C 33.41 % H 3.10 % N 2.51 % Cr 2.33 % Mo 25.86 % Y 3.99 %; found: C 33.52 %, H 3.18 %, N 2.62 %, Cr 2.01 %, Mo 25.50 %, Y 3.66 %.

## 3. Crystallographic data and structure refinements

**Table S1 Crystallographic data**

| Name | POMOF-1 |
|---|---|
| Empirical formula | C62 H87 O49 Cr Mo6 N4 Y |
| Formula weight | 2388.90 |
| Temperature (K) | 150.0 |
| Wave length (Å) | 0.71073 |
| Crystal system | Triclinic |
| Space group | *P* -1 |
| a (Å) | 13.262(2) |
| b (Å) | 13.818(3) |
| c (Å) | 24.319(4) |
| α (deg) | 104.555(7) |
| β (deg) | 104.167(7) |
| γ (deg) | 90.510(6) |
| Volume ($Å^3$) | 4170.5(13) |
| Z | 2 |
| Dcalc ($Mg/m^3$) | 1.902 |
| Absorption coefficient ($mm^{-1}$) | 1.790 |
| F (000) | 2388 |
| θ range (deg) | 1.961 - 25.355 |
| index range (deg) | -15<h<14, -16<k<16, -29<l<29 |
| Data completeness | 99.9% |
| Reflections collected / unique | 78679/ 15210 [R(int) = 0.1096] |
| Data / restraints / parameters | 15210/1638/1009 |
| Goodness-of-fit on $F^2$ | 1.051 |
| $R_1$, $wR_2$ ($I > 2\sigma(I)$) | $R_1 = 0.0536$, $wR_2 = 0.1415$ |
| $R_1$, $wR_2$ (all data) | $R_1 = 0.0771$, $wR_2 = 0.1558$ |
| Largest diff. peak and hole ($e\ Å^{-3}$) | 2.980, -0.853 |

$R_1 = \Sigma||Fo|-|Fc||/\ \Sigma|Fo|$. $wR_2 = [\Sigma[\ w\ (Fo^2-Fc^{\ 2})^2] / \Sigma[\ w\ (Fo^{\ 2})^2]]^{1/2}$

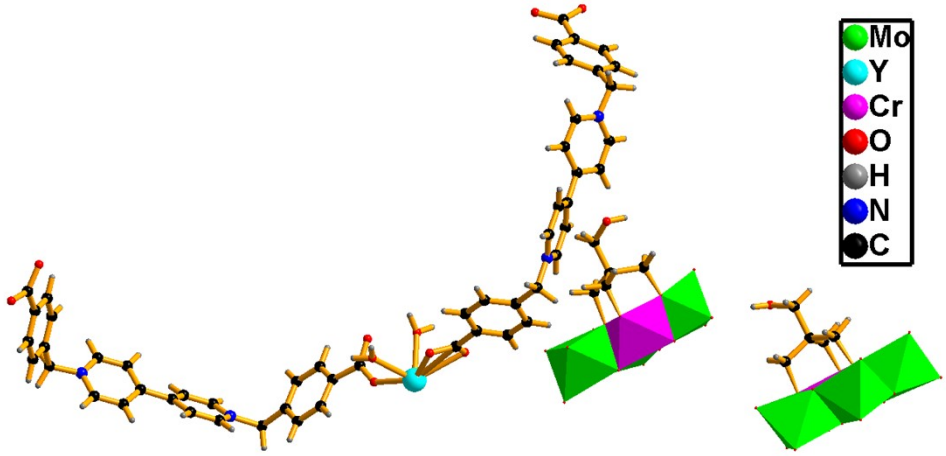


**Figure S1**. Asymmetric unit of **POMOF-1** (Colour Scheme: Mo: bright green polyhedron; Cr: pink polyhedron; Y: cyan; O: red; H: gray; N: light blue; C: black)

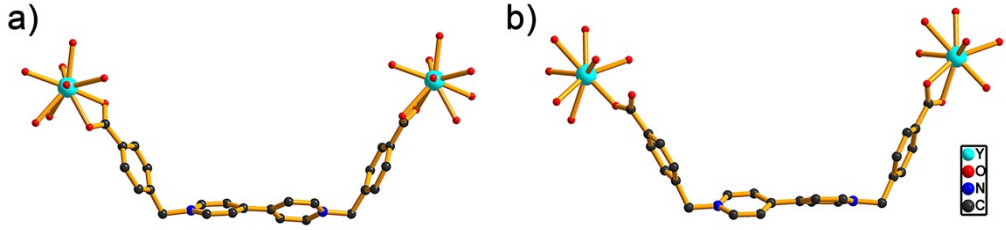


**Figure S2.** Two kinds of coordinating modes of **L** in **POMOF-1** (Colour Scheme: Y: cyan; O: red; N: light blue; C: black)

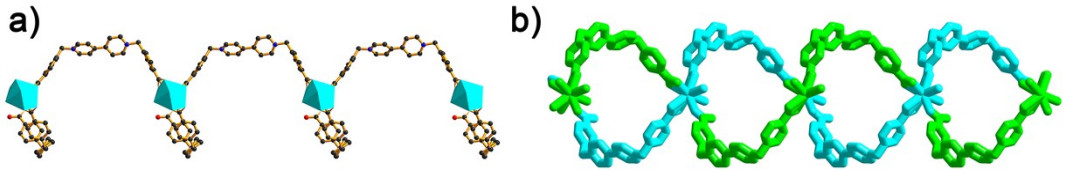


**Figure S3. a)** Side view of cationic 2D single network, **b)** Top view of cationic 2D single network along *b* axis.

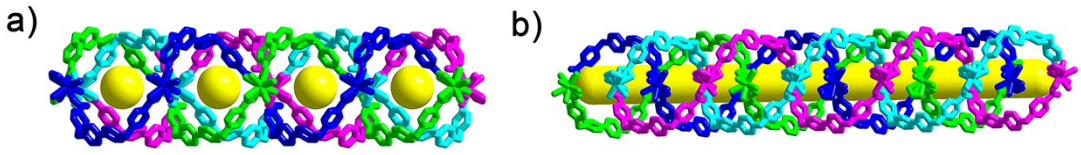

**Figure S4**. View of the 1D open channels along **a)** *b* axis and **b)** a axis.

## 4. Characterization of POMOF-1

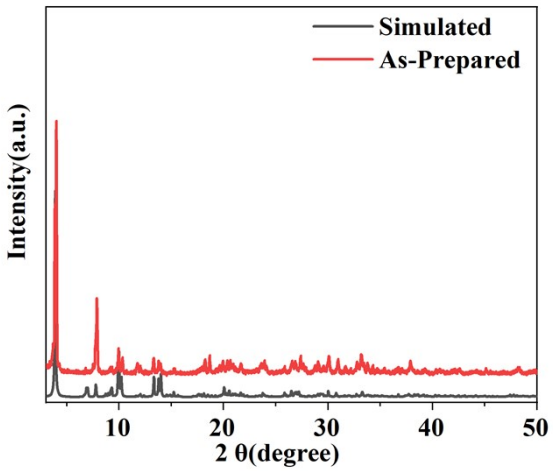


**Figure S5.** PXRD pattern of **POMOF-1**

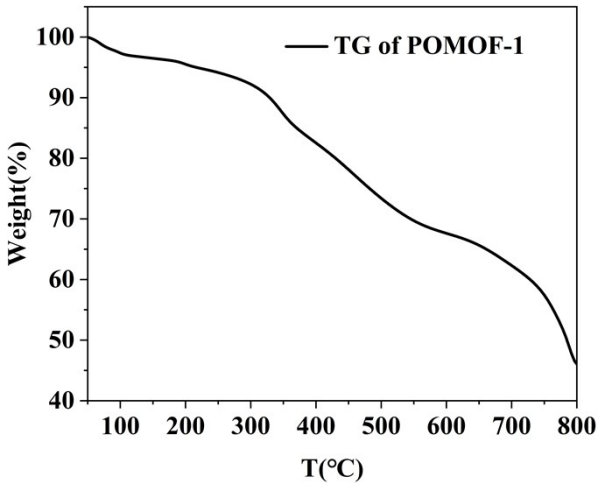


**Figure S6**. The TGA Curve of **POMOF-1**

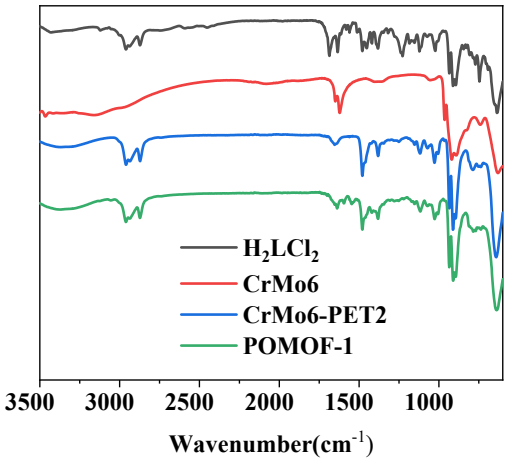


**Figure S7**. The FT-IR spectra of $H_2LCl_2$, **CrMo6**, **CrMo6-PET2** and **POMOF-1**

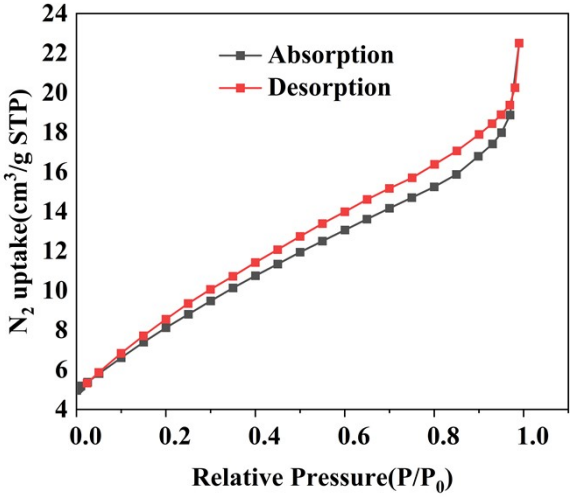


**Figure S8.** The $N_2$ absorption / desorption isotherms of **POMOF-1** at 77K ($P_0$ = 101 kPa) with BET surface area of 29.968 $m^2g^{-1}$

## 5. Catalytic performance of POMOF-1

**General methods for N-formylation of amines. POMOF-1** (0.1 mol%), amines **1** (1 mmol), $CH_3OH$ (1 mL) and 30% $H_2O_2$ (4 mmol) were added into seal tube. Then the reaction was heated at 80 °C and stirring for 2 h. The reactor was cool down to room temperature, the catalyst was centrifuged and the supernatant was diluted with ethyl acetate. The conversion of amines **1** and yields of product formamides **2** were determined by gas chromatography-mass spectrometry (GC-MS). Then, the reaction was quenched with $H_2O$ and extracted with ethyl acetate. Filtering out the insoluble substances, the organic phases were washed with $H_2O$, and dried over anhydrous $Na_2SO_4$. The organic phases were filtered and concentrated under reduced pressure and the crude products were purified by silica gel column chromatography (eluent: ethyl acetate-petroleum ether, 1: 1~5) to yield the pure products. The products were

characterized by $^{1}H$ NMR, $^{13}C$ NMR analyses.

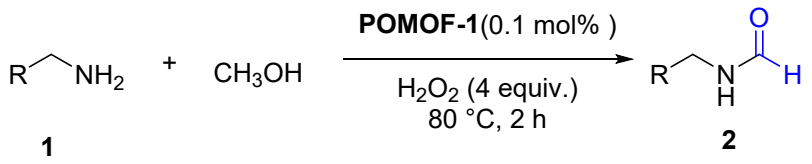


**Table S2**. Optimization for N-formylation reaction condition of benzylamine(**1a**) with **POMOF-1**

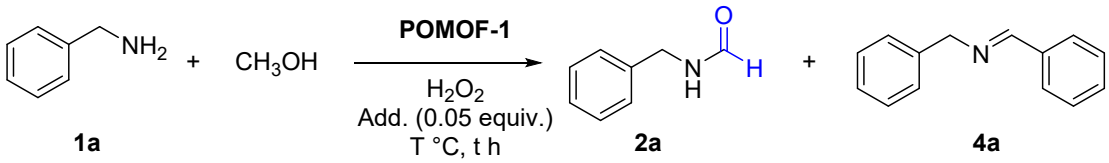


| Entry | **POMOF-1** | $H_2O_2$ | Add. | T/°C | t/h | Yields% | |
|---|---|---|---|---|---|---|---|
| | | | | | | 2a | 4a |
| 1 | 0.1 mol% | 4 mmol | $Na_2SO_3$ | 80 | 2 | 75 | 15 |
| 2 | 0.1 mol% | 4 mmol | $Na_2S_2O_3$ | 80 | 2 | 45 | 35 |
| 3 | 0.1 mol% | 4 mmol | $Na_2S_2O_4$ | 80 | 2 | 42 | 37 |
| 4 | 0.1 mol% | 4 mmol | None | 80 | 2 | 95 | trace |
| 5 | 0.1 mol% | 4 mmol | None | 80 | 0.3 | 35 | trace |
| 6 | 0.1 mol% | 4 mmol | None | 80 | 1 | 70 | trace |
| 7 | 0.1 mol% | 4 mmol | None | 80 | 1.5 | 85 | trace |
| 8 | 0.1 mol% | 1 mmol | None | 80 | 2 | 20 | 30 |
| 9 | 0.1 mol% | 2 mmol | None | 80 | 2 | 25 | 35 |
| 10 | 0.1 mol% | 3 mmol | None | 80 | 2 | 65 | 30 |
| 11 | 0.05 mol% | 4 mmol | None | 80 | 2 | 84 | 7 |
| 12 | 0.1 mol% | 4 mmol | None | 60 | 2 | 15 | 25 |
| 13 | 0.1 mol% | 4 mmol | None | 40 | 2 | trace | 15 |

Reaction condition: **POMOF-1,** $CH_3OH$ (1 mL), benzylamine **1a** (1 mmol) and 30% $H_2O_2$ at 80 °C. Yields were determined by GC-MS.

**Table S3.** Oxidant selective experiments for N-formylation reaction of benzylamine (**1a**) with **POMOF-1**

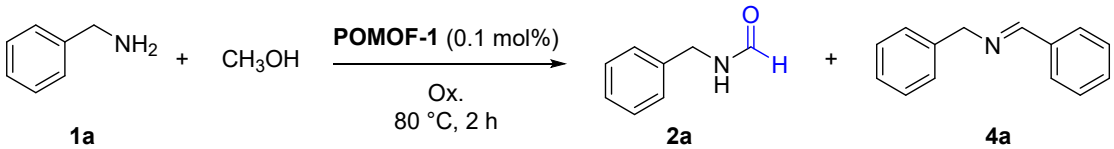


| Entry | Ox. | Yields% | |
|---|---|---|---|
| | | 2a | 4a |
| 1 | 4 mmol TBHP | 0 | 90 |
| 2 | 4 mmol DTBP | 0 | 70 |

| | | | |
|---|---|---|---|
| 3 | 4 mmol BPO | 0 | 0 |
| 4[a] | None | trace | 13 |
| 5[b] | None | trace | 8 |
| 6[c] | None | trace | trace |

Reaction condition: **POMOF-1** (0.1 mol%), $CH_3OH$ (1 mL), benzylamine **1a** (1 mmol) and Oxidant at 80 °C. Yields were determined by GC-MS. [a]Reaction was under $O_2$ atmosphere. [b]Reaction was under air atmosphere. [c]Reaction was under $N_2$ atmosphere.

**General methods for oxidation coupling reaction of arylmethanamines. POMOF-1** (0.1 mol%), arylmethylamines **1** (1 mmol), diphenyl ether (1 mL) and 30% $H_2O_2$ (1.5 mmol) were added into seal tube. The mixture was heated at 80 °C and stirring for 8 h. The reactor was cool down to room temperature, the catalyst was centrifuged and the supernatant was diluted with ethyl acetate. The conversion of arylmethylamines **1** and yields of product imines **4** were determined by gas chromatography-mass spectrometry (GC-MS). Then, the reaction was quenched with $H_2O$ and extracted with ethyl acetate. Filtering out the insoluble substances, the organic phases were washed with $H_2O$, and dried over anhydrous $Na_2SO_4$. The organic phases were filtered and concentrated under reduced pressure and the crude products were purified by silica gel column chromatography (eluent: ethyl acetate-petroleum ether, 1:10 ~50) to yield the pure products. The products were characterized by $^1H$ NMR, $^{13}C$ NMR analyses.

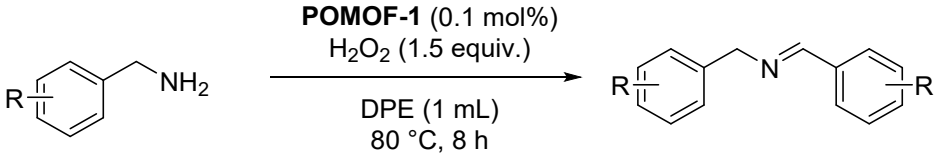


**1** **4**

**Table S4**. Optimization for oxidation coupling reaction of benzylamine (**1a**) with **POMOF-1**

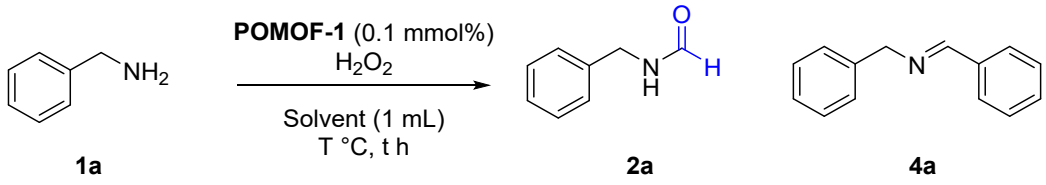


**1a** **2a** **4a**

| Entry | Solvent | $H_2O_2$ | T/°C | t/h | Yields% | |
|---|---|---|---|---|---|---|
| | | | | | **2a** | **4a** |
| 1 | $H_2O$ | 1.5 mmol | 60 | 8 | trace | 62 |
| 2 | $CH_3CN$ | 1.5 mmol | 60 | 8 | trace | 41 |
| 3 | DCE | 1.5 mmol | 60 | 8 | trace | 72 |
| 4 | Dioxane | 1.5 mmol | 60 | 8 | trace | 75 |
| 5 | DME | 1.5 mmol | 60 | 8 | trace | 77 |
| 6 | MTBE | 1.5 mmol | 60 | 8 | trace | 79 |
| 7 | THF | 1.5 mmol | 60 | 8 | trace | 80 |
| 8 | DPE | 1.5 mmol | 60 | 8 | trace | 88 |
| 9 | DPE | 1.5 mmol | 80 | 8 | trace | 97 |

**Reaction condition**: **POMOF-1** (0.1 mol%), solvent (1 mL), benzylamine **1a** (1 mmol) and 30% $H_2O_2$ at 80 °C. Yields were determined by GC-MS.

**General methods for oxidation of Anilines. POMOF-1** (0.1% mmol), $Na_2S_2O_4$ (0.05 mmol), arylamines **5** (1 mmol), dichloroethane (1 mL), and $H_2O_2$ (2.5 mmol) were added into seal tube. The mixture was heated at 80 °C and stirring for 8 h. The reactor was cool down to room temperature, the catalyst was centrifuged and the supernatant was diluted with ethyl acetate. The conversion of arylamines **5** and yields of product azobenzenes **6** were determined by gas chromatography-mass spectrometry (GC-MS). Then, the reaction was quenched with $H_2O$ and extracted with ethyl acetate. Filtering out the insoluble substances, the organic phases were washed with $H_2O$, and dried over anhydrous $Na_2SO_4$. The organic phases were filtered and concentrated under reduced pressure and the crude products were purified by silica gel column chromatography (eluent: ethyl acetate-petroleum ether, 1:100-500) to yield the pure products. The products were characterized by $^1H$ NMR, $^{13}C$ NMR analyses.

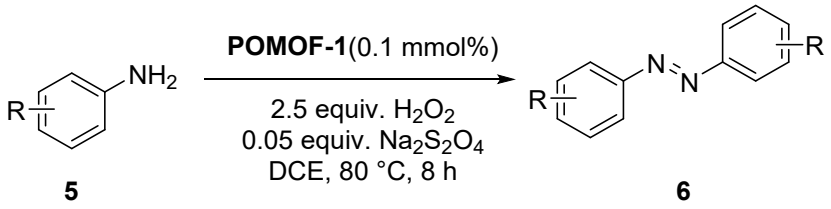


**Table S5.** Optimization for oxidation coupling reaction of Aniline (**5a**) with **POMOF-1**

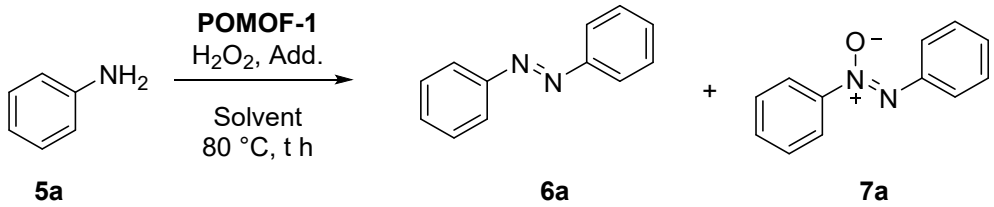


| Entry | Solvent | $H_2O_2$ | Add. | t/h | Yields% | |
|---|---|---|---|---|---|---|
| | | | | | 6a | 7a |
| 1 | $CH_3OH$ | 4 mmol | None | 2 | 15 | 12 |
| 2 | $CH_3OH$ | 4 mmol | None | 4 | 27 | 31 |
| 3 | $CH_3OH$ | 4 mmol | None | 8 | 36 | 37 |
| 4 | $CH_3OH$ | 4 mmol | None | 12 | 32 | 45 |
| 5 | $CH_3OH$ | 4 mmol | 0.05 equiv. $Na_2SO_3$ | 8 | 20 | 15 |
| 6 | $CH_3OH$ | 4 mmol | 0.05 equiv. $Na_2S_2O_3$ | 8 | 55 | 32 |
| 7 | $CH_3OH$ | 4 mmol | 0.05 equiv. $Na_2S_2O_4$ | 8 | 60 | 18 |
| 8 | EtOH | 4 mmol | 0.05 equiv. $Na_2S_2O_4$ | 8 | 52 | 17 |
| 9 | DMSO | 4 mmol | 0.05 equiv. $Na_2S_2O_4$ | 8 | trace | trace |
| 10 | DMF | 4 mmol | 0.05 equiv. $Na_2S_2O_4$ | 8 | trace | trace |
| 11 | $CH_3CN$ | 4 mmol | 0.05 equiv. $Na_2S_2O_4$ | 8 | 20 | 7 |
| 12 | Toluene | 4 mmol | 0.05 equiv. $Na_2S_2O_4$ | 8 | 50 | trace |
| 13 | THF | 4 mmol | 0.05 equiv. $Na_2S_2O_4$ | 8 | 16 | trace |
| 14 | Acetone | 4 mmol | 0.05 equiv. $Na_2S_2O_4$ | 8 | 12 | trace |
| 15 | DCM | 4 mmol | 0.05 equiv. $Na_2S_2O_4$ | 8 | 62 | 18 |
| 16 | DCE | 4 mmol | 0.05 equiv. $Na_2S_2O_4$ | 8 | 70 | 22 |

| | | | | | | |
|---|---|---|---|---|---|---|
| 17 | DCE | 1 mmol | 0.05 equiv. $Na_2S_2O_4$ | 8 | 34 | 7 |
| 18 | DCE | 2 mmol | 0.05 equiv. $Na_2S_2O_4$ | 8 | 56 | 8 |
| 19 | DCE | 3 mmol | 0.05 equiv. $Na_2S_2O_4$ | 8 | 75 | 15 |
| 20 | DCE | 2.5 mmol | 0.05 equiv. $Na_2S_2O_4$ | 8 | 86 | 5 |
| 21[a] | DCE | 2.5 mmol | 0.05 equiv. $Na_2S_2O_4$ | 8 | 57 | 11 |
| 22[b] | DCE | 2.5 mmol | 0.05 equiv. $Na_2S_2O_4$ | 8 | 71 | Trace |
| 23 | DCE | 2.5 mmol | None | 8 | 30 | 34 |
| 24 | DCE | 2 mmol | None | 8 | 21 | 24 |
| 25 | DCE | 1 mmol | None | 8 | 14 | 13 |

**Reaction condition**: **POMOF-1** (0.1 mol%), additive, solvent (1 mL), aniline **5a** (1 mmol) and 30% $H_2O_2$ at 80 °C. Yields were determined by GC-MS. [a] temperature: 100 °C. [b] temperature: 60 °C

## 6. Recycling experiment of POMOF-1.

The reusability of the catalyst **POMOF-1** was tested using benzylamine (**1a**) as the substrate. After the completion of the first catalytic reaction, the catalyst was recovered by filtration and then washed with $CH_3OH$ and Acetone. The recovered **POMOF-1** was dried under vacuum and reused for the next run under the same conditions.

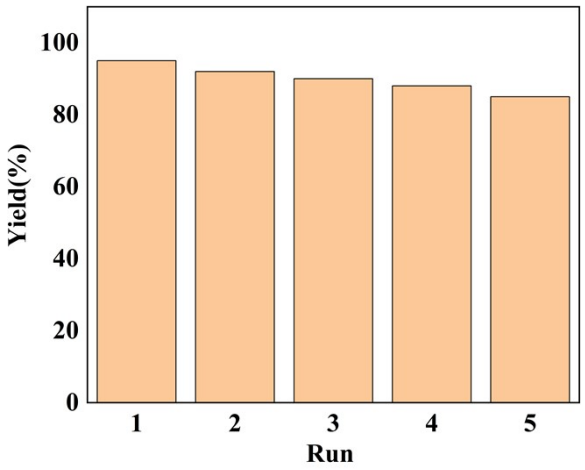


**Figure S9.** The recyclability of **POMOF-1.**

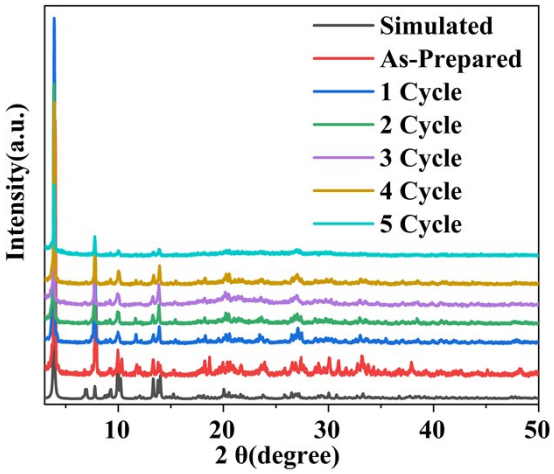


**Figure S10.** PXRD patterns of the recovered catalyst **POMOF-1** after 5 cycles.

**Table S6**. ICP Analysis of **POMOF-1** after catalysis.

| Element | Y | Cr | Mo |
|---|---|---|---|
| Calculated Value (%) | 3.99 | 2.33 | 25.86 |
| Actual value (%) | 3.66 | 2.01 | 25.50 |
| After catalysis (%) | 3.54 | 1.98 | 25.41 |
| Mother liquor after catalyst filtration (%) | < 0.01 | < 0.01 | < 0.01 |
| Mother liquor after hot filtration (%) | < 0.01 | < 0.01 | < 0.01 |

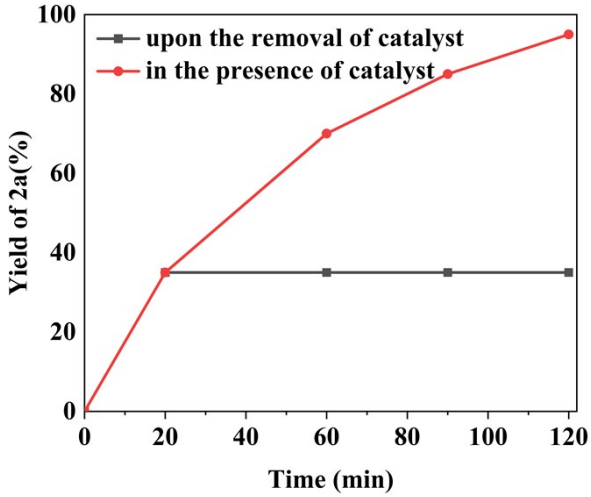


**Figure S11.** Hot filtration test for N-formylation reaction of benzylamine (**1a**), red: **POMOF-1** as the catalyst during the reaction, black: the catalyst was filtered out during the reaction

## 7. Mechanism study

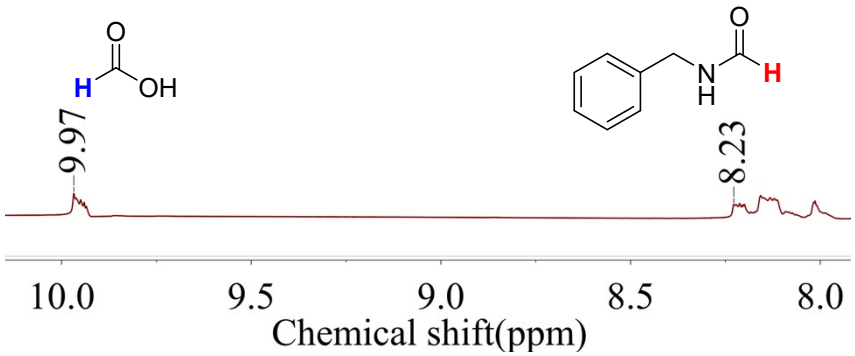


**Figure S12.** $^{1}$H NMR of N-formylation reaction at 20 min.

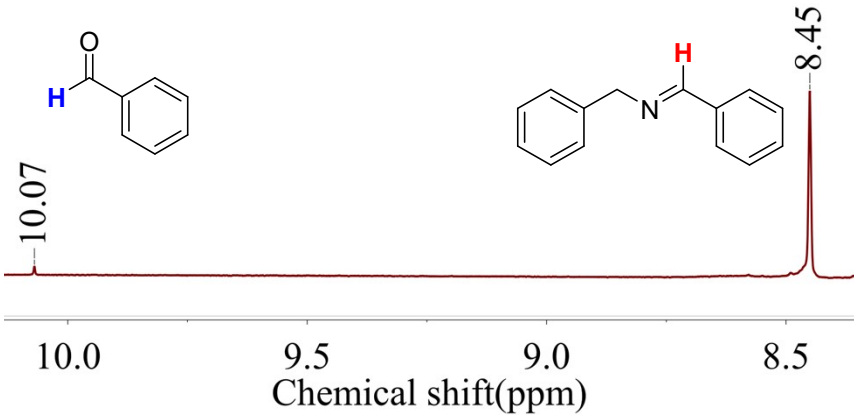


**Figure S13.** $^{1}$H NMR of oxidative coupling reaction of arylmethylamine at 1 h.

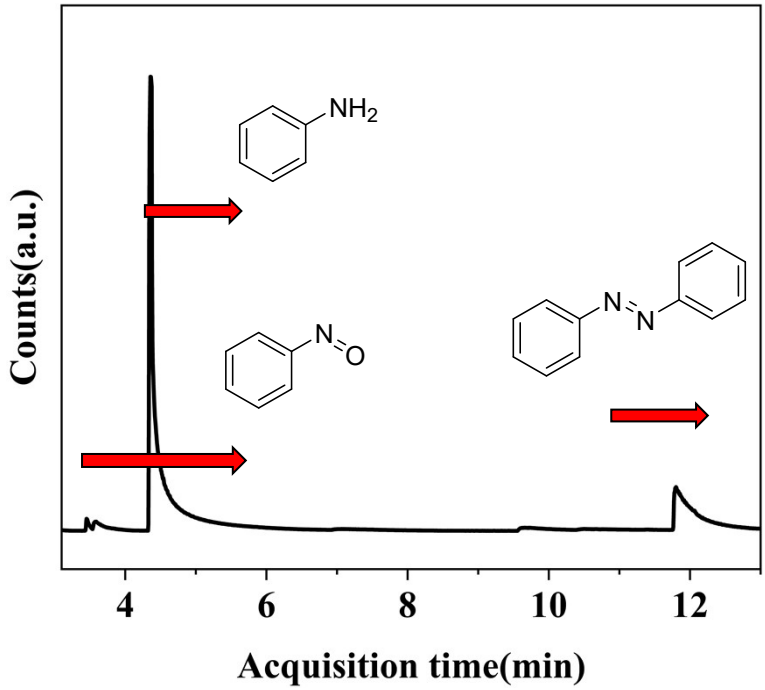


**Figure S14** GC spectrum of oxidative coupling reaction of aniline at 2 h.

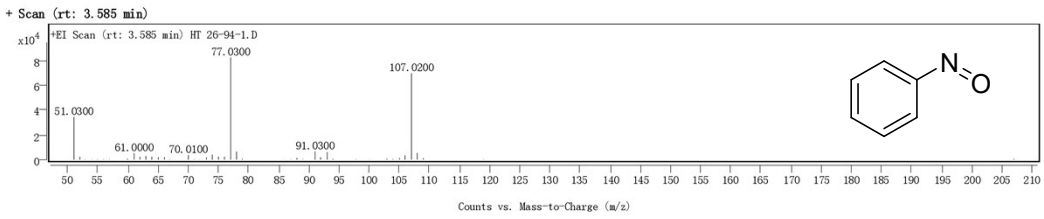

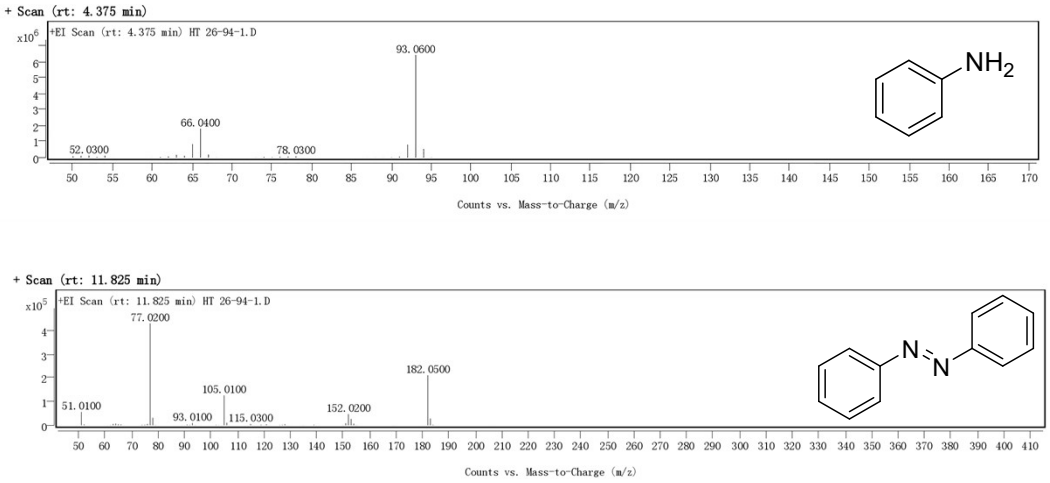


**Figure S15.** MS spectra of oxidative coupling reaction of aniline at 2 h.

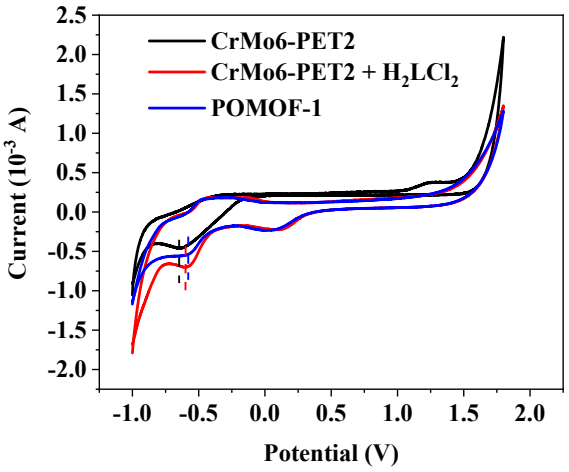


**Figure S16.** CV study of CrMo6-PET2, **POMOF-1** and mixture of CrMo6-PET2 and $H_2LCl_2$ at 50 mV/s in 1 M $Na_2SO_4$ solution.

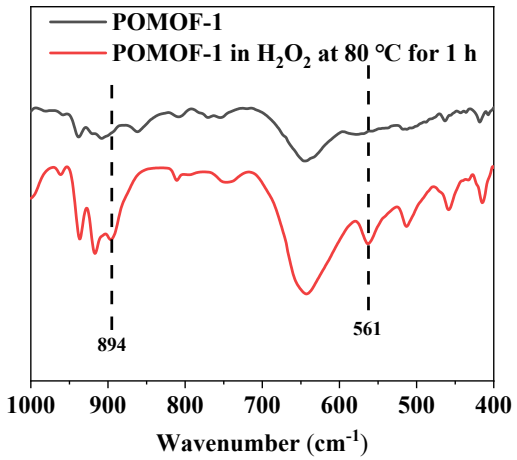


**Figure S17**. FI-IR spectrum of **POMOF-1** in $H_2O_2$ at 80 °C for 1 h. The bands centered at 894 $cm^{-1}$ and 561 $cm^{-1}$ are ascribed to ν(O-O) and ν(Mo($O_2$)).

## 8. Characterization of products

**N-benzylformamide(2a)**.[6] Light yellow solid. Yield: 85%, $^{1}$H NMR (600 MHz, $CDCl_3$) δ 8.29 (s, 1H), 7.39 - 7.35 (m, 2H), 7.32 (m, 3H), 5.97 (s, 1H), 4.51 (d, $J$ = 5.8 Hz, 2H). $^{13}$C NMR (151 MHz, $CDCl_3$) δ 161.04, 137.47, 128.82, 127.83, 127.76, 42.27.

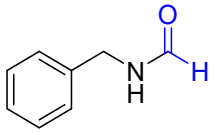

**N-(4-methylbenzyl)formamide(2b)**.[6] Light yellow solid. Yield: 82%. $^{1}$H NMR (600 MHz, $CDCl_3$) δ 8.24 (s, 1H), 7.19 (d, $J$ = 7.9 Hz, 2H), 7.16 (d, $J$ = 8.1 Hz, 2H), 6.05 (s, 1H), 4.44 (d, $J$ = 5.9 Hz, 2H), 2.35 (s, 3H). $^{13}$C NMR (151 MHz, $CDCl_3$) δ 161.01, 137.43, 134.56, 129.44, 127.80, 41.95, 21.11.

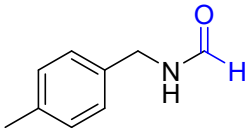

**N-(3-methylbenzyl)formamide(2c)**.[6] Light yellow solid. Yield: 83%. $^{1}$H NMR (600 MHz, $CDCl_3$) δ 8.28 (s, 1H), 7.29-7.24 (m, 1H), 7.14 -7.10 (m, 3H), 6.01 (s, 1H), 4.47 (d, $J$ = 5.8 Hz, 2H), 2.36 (s, 3H). $^{13}$C NMR (151 MHz, $CDCl_3$) δ 161.05, 138.57, 137.38, 128.71, 128.58, 128.47, 124.83, 42.23, 21.36.

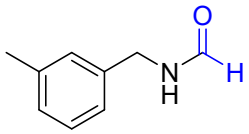

**N-(2-methylbenzyl)formamide(2d)**.[6] Light yellow solid. Yield: 83%. $^{1}$H NMR (600 MHz, $CDCl_3$) δ 8.28 (s, 1H), 7.26 - 7.21 (m, 4H), 5.67 (s, 1H), 4.52 (d, $J$ = 5.5 Hz, 2H), 2.36 (s, 3H). $^{13}$C NMR (151 MHz, $CDCl_3$) δ 160.83, 136.47, 135.06, 130.66, 128.62, 128.06, 126.34, 40.42, 19.02.

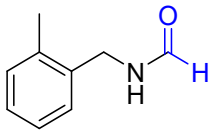

**N-(4-chlorobenzyl)formamide(2e)**.[6] Light yellow solid. Yields: 85%. $^{1}$H NMR (600 MHz, $CDCl_3$) δ 8.29 (s, 1H), 7.35 - 7.31 (m, 2H), 7.26 - 7.23 (m, 2H), 5.96 (s, 1H), 4.48 (d, $J$ = 6.0 Hz, 2H). $^{13}$C NMR (151 MHz, $CDCl_3$) δ 160.98, 136.11, 133.56, 129.14, 128.93, 41.50.

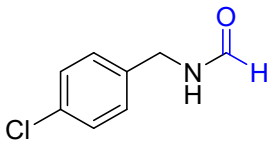

**N-(4-methoxybenzyl)formamide(2f)**.[6] Light yellow solid. Yields: 91%. $^{1}$H NMR (600 MHz, $CDCl_3$) δ 8.25 (s, 1H), 7.24 (d, *J* = 8.5 Hz, 2H), 6.89 (d, *J* = 8.6 Hz, 2H), 5.87 (s, 1H), 4.43 (d, *J* = 5.8 Hz, 2H), 3.82 (s, 3H). $^{13}$C NMR (151 MHz, $CDCl_3$) δ 160.89, 129.65, 129.21, 128.32, 114.16, 77.25, 77.04, 76.83, 55.33, 41.70.

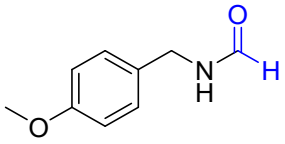

**N-(1-phenylethyl)formamide(2g)**.[6] Light yellow oil. Yields: 55%. $^{1}$H NMR (600 MHz, $CDCl_3$) δ 8.03 (s, 1H), 7.34 - 7.29 (m, 4H), 7.27 - 7.24 (m, 1H), 5.13 (p, *J* = 7.2 Hz, 1H), 1.46 (d, *J* = 7.0 Hz, 3H). $^{13}$C NMR (151 MHz, $CDCl_3$) δ 160.50, 142.70, 128.70, 127.47, 126.13, 47.62, 21.82.

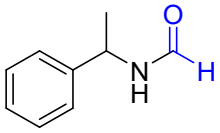

**N-(naphthalen-2-ylmethyl)formamide(2h)**.[6] Light yellow solid. Yield: 69%. $^{1}$H NMR (600 MHz, $CDCl_3$) δ 8.32 (s, 1H), 7.86 - 7.82 (m, 3H), 7.74 (s, 1H), 7.52 - 7.49 (m, 2H), 7.41 (dd, *J* = 8.4, 1.7 Hz, 1H), 6.06 (s, 1H), 4.65 (d, *J* = 5.9 Hz, 2H). $^{13}$C NMR (151 MHz, $CDCl_3$) δ 161.07, 134.96, 133.32, 132.80, 128.68, 127.72, 126.49, 126.42, 126.11, 125.77, 42.32.

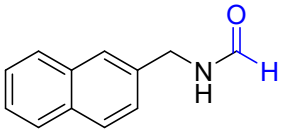

**N-(pyridin-4-ylmethyl)formamide(2i)**.[7] Yield: 51%. Yellow oil. $^{1}$H NMR (600 MHz, $CDCl_3$) δ 8.48 - 8.46 (m, 2H), 8.27 (d, *J* = 1.5 Hz, 1H), 7.18 - 7.17 (m, 2H), 4.46 - 4.44 (m, 2H).$^{13}$C NMR (151 MHz, $CDCl_3$) δ 161.60, 149.75, 147.14, 122.31, 40.85.

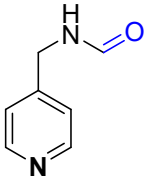

**N-(thiophen-2-ylmethyl)formamide(2j).**[6] Yield: 61%. Yellow oil. $^{1}$H NMR (600 MHz, $CDCl_3$) δ 8.09 (d, *J* = 1.7 Hz, 1H), 7.19-7.18 (m, 1H), 7.12 - 7.03 (m, 1H), 6.94 - 6.92 (m, 1H), 6.92 - 6.89 (m, 1H) 4.55 (d, *J* = 6.0 Hz, 2H). $^{13}$C NMR (151 MHz,

$CDCl_3$) δ 161.36, 140.37, 126.93, 126.10, 125.22, 36.77.

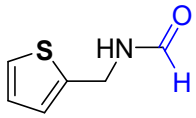

**N-cyclohexylformamide(2k)**.[6] Yields: 73%. $^1$H NMR (600 MHz, $CDCl_3$) δ 8.05 (s, 1H), 6.15 (s, 1H), 3.80 (dt, *J* = 7.6, 3.5 Hz, 1H), 1.88 (dt, *J* = 12.7, 4.1 Hz, 2H), 1.68 (dt, *J* = 13.5, 4.0 Hz, 2H), 1.60 - 1.57 (m, 1H), 1.33 - 1.28 (m, 2H), 1.15 (td, *J* = 12.0, 3.8 Hz, 3H). $^{13}$C NMR (151 MHz, $CDCl_3$) δ 160.53, 47.08, 32.92, 25.39, 24.73.

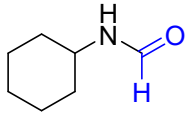

**N-pentylformamide(2l)**.[8] Yield: 95%. Yellow oil. $^1$H NMR (600 MHz, $CDCl_3$) δ 8.12 (s, 1H), 6.36 (s, 1H), 3.24 (q, *J* = 6.8 Hz, 2H), 1.52 - 1.48 (m, 2H), 1.32 -1.27 (m, 4H), 0.87 (t, *J* = 6.7 Hz, 3H). $^{13}$C NMR (151 MHz, $CDCl_3$) δ 161.53, 38.15, 29.03, 28.91, 22.22, 13.87.

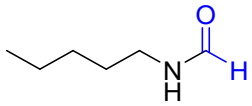

**N-benzyl-1-phenylmethanimine(4a).**[9] Yield: 88%. 1H NMR (600 MHz, $CDCl_3$) δ 8.45 (s, 1H), 7.84 (d, J = 7.1 Hz, 2H), 7.47 (s, 3H), 7.40 (d, J = 4.3 Hz, 4H), 7.34 -7.30 (m, 1H), 4.88 (s, 2H). 13C NMR (151 MHz, $CDCl_3$) δ 162.10, 139.30, 136.16, 130.83, 128.65, 128.54, 128.34, 128.04, 127.04, 65.08.

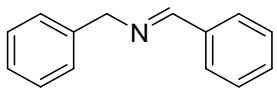

**N-(4-methylbenzyl)-1-(p-tolyl)methanimine(4b)**. [9] Yield: 85%. White oil. $^1$H NMR (600 MHz, $CDCl_3$) δ 7.86 - 7.81 (m, 2H), 7.33 (d, *J* = 8.1 Hz, 2H), 2.46 (s, 3H). $^{13}$C NMR (151 MHz, $CDCl_3$) δ 161.72, 143.56, 140.99, 136.51, 136.38, 133.65, 131.70, 129.76, 129.33, 129.18, 128.31, 128.28, 127.99, 126.28, 64.83, 27.47, 21.54, 21.14.

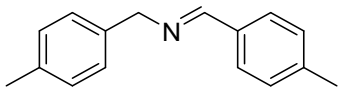

**N-(3-methylbenzyl)-1-(m-tolyl)methanimine(4c)**. [9] Yield: 91%. $^1$H NMR (600 MHz, $CDCl_3$) δ 8.39 (d, *J* = 1.4 Hz, 1H), 7.69 (s, 1H), 7.58 (d, *J* = 7.6 Hz, 1H), 7.34 (t, *J* = 7.6 Hz, 1H), 7.29 – 7.25 (m, 2H), 7.19 - 7.15 (m, 2H), 7.11 (d, *J* = 7.5 Hz, 1H), 4.82 (d, *J* = 1.3 Hz, 2H), 2.42 (s, 3H), 2.38 (s, 3H). $^{13}$C NMR (151 MHz, $CDCl_3$) δ 162.18, 139.15, 138.36, 138.14, 136.11, 131.60, 128.79, 128.50, 128.41, 127.76, 125.88, 125.10, 65.16, 21.45.

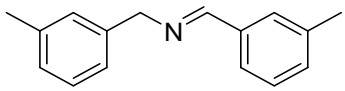

**N-(2-methylbenzyl)-1-(o-tolyl)methanimine(4d)**.[9] Yield: 81%. $^{1}$H NMR (600 MHz, $CDCl_3$) δ 8.73 (s, 1H), 7.99 (d, *J* = 7.8 Hz, 1H), 7.38 - 7.34 (m, 2H), 7.30 (d, *J* = 7.5 Hz, 1H), 7.25 (t, *J* = 3.1 Hz, 3H), 4.89 (s, 2H), 2.57 (d, *J* = 2.5 Hz, 3H), 2.46 (d, *J* = 2.5 Hz, 3H). $^{13}$C NMR (151 MHz, $CDCl_3$) δ 160.62, 137.75, 137.67, 136.16, 134.27, 130.86, 130.31, 130.17, 128.34, 127.74, 127.10, 126.23, 126.12, 63.34, 19.45, 19.35.

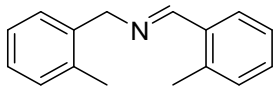

**N-(4-chlorobenzyl)-1-(4-chlorophenyl)methanimine(4e)**.[9] Yield: 94%. Pale yellow oil. $^{1}$H NMR (600 MHz, $CDCl_3$) δ 8.37 (d, *J* = 1.5 Hz, 1H), 7.77 - 7.72 (m, 2H), 7.44 - 7.40 (m, 2H), 7.34 (d, *J* = 8.5 Hz, 2H), 7.29 (d, *J* = 7.9 Hz, 2H), 4.79 (s, 2H).
$^{13}$C NMR (151 MHz, $CDCl_3$) δ 160.89, 137.59, 136.91, 134.44, 132.84, 129.48, 129.28, 128.95, 128.65, 64.17.

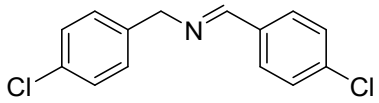

**N-(4-methoxybenzyl)-1-(4-methoxyphenyl)methanimine(4f)**.[9] Yield: 85%. Difficult to isolate.

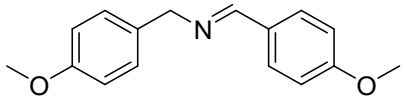

**1,2-diphenyldiazene(6a)**.[10] Orange solid. Yield: 80%. $^{1}$H NMR (600 MHz, $CDCl_3$) δ 8.00 - 7.95 (m, 2H), 7.59 - 7.54 (m, 2H), 7.54 - 7.49 (m, 1H). $^{13}$C NMR (151 MHz, $CDCl_3$) δ 152.66, 131.00, 129.10, 122.85.

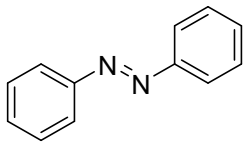

**1,2-di-p-tolylethene(6b)**.[10] Orange solid. Yield: 85%. $^{1}$H NMR (600 MHz, $CDCl_3$) δ 7.86 - 7.81 (m, 2H), 7.33 (d, *J* = 8.0 Hz, 2H), 2.46 (s, 3H). $^{13}$C NMR (151 MHz, $CDCl_3$) δ 150.82, 141.21, 129.71, 122.72, 21.49.

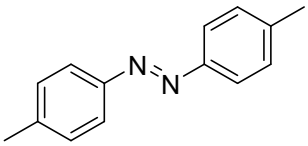

**1,2-bis(4-methoxyphenyl)diazene(6c)**.[10] Orange solid. Yield: 92%. $^{1}$H NMR (600 MHz, $CDCl_3$) δ 7.94 - 7.88 (m, 2H), 7.05 - 7.01 (m, 2H), 3.91 (s, 3H). $^{13}$C NMR (151 MHz, $CDCl_3$) δ 161.56, 147.08, 124.34, 114.17, 55.57.

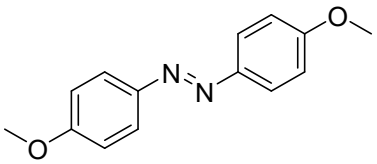

**1,2-bis(3-methoxyphenyl)diazene(6d)**.[10] Orange solid. Yield: 65%. $^{1}$H NMR (600 MHz, $CDCl_3$) δ 7.6 - 7.57 (m, 1H), 7.48 (dd, $J$ = 2.6, 1.7 Hz, 1H), 7.46 (t, $J$ = 8.0 Hz, 1H), 7.09 – 7.06 (m, 1H), 3.93 (s, 3H). $^{13}$C NMR (151 MHz, $CDCl_3$) δ 160.32, 153.81, 129.79, 117.89, 117.17, 105.71, 55.50.

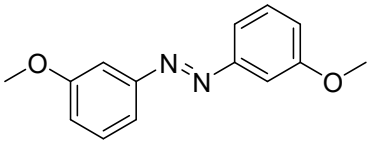

**1,2-bis(2-methoxyphenyl)diazene(6e)**.[10] Orange solid. Yield: 80%. $^{1}$H NMR (600 MHz, $CDCl_3$) δ 7.65 (dd, $J$ = 7.9, 1.7 Hz, 1H), 7.46 - 7.42 (m, 1H), 7.10 (dd, $J$ = 8.3, 1.2 Hz, 1H), 7.05 - 7.07 (m, 1H), 4.04 (s, 3H). $^{13}$C NMR (151 MHz, $CDCl_3$) δ 156.83, 142.95, 132.20, 120.82, 117.54, 112.52, 56.33.

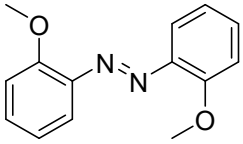

**1,2-bis(4-chlorophenyl)diazene(6f).**[10] Orange solid. Yield: 69%. $^{1}$H NMR (600 MHz, $CDCl_3$) δ 7.91 - 7.87 (m, 2H), 7.54 - 7.49 (m, 2H). $^{13}$C NMR (151 MHz, $CDCl_3$) δ 150.79, 137.24, 129.41, 124.20.

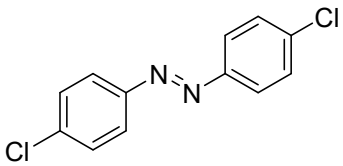

**1,1'-(diazene-1,2-diylbis(4,1-phenylene))bis(ethan-1-one)(6g)**.[11] Orange solid. Yield: 30%. $^{1}$H NMR (600 MHz, $CDCl_3$) δ 8.17 - 8.14 (m, 2H), 8.05 - 8.03 (m, 2H), 2.71 (s, 3H). $^{13}$C NMR (151 MHz, $CDCl_3$) δ 197.40, 154.83, 138.92, 129.43, 123.22,

26.90.

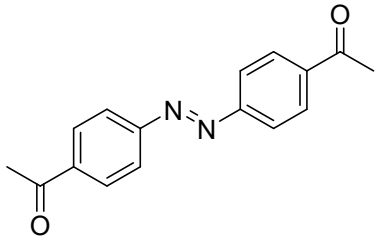


## 9. NMR spectra

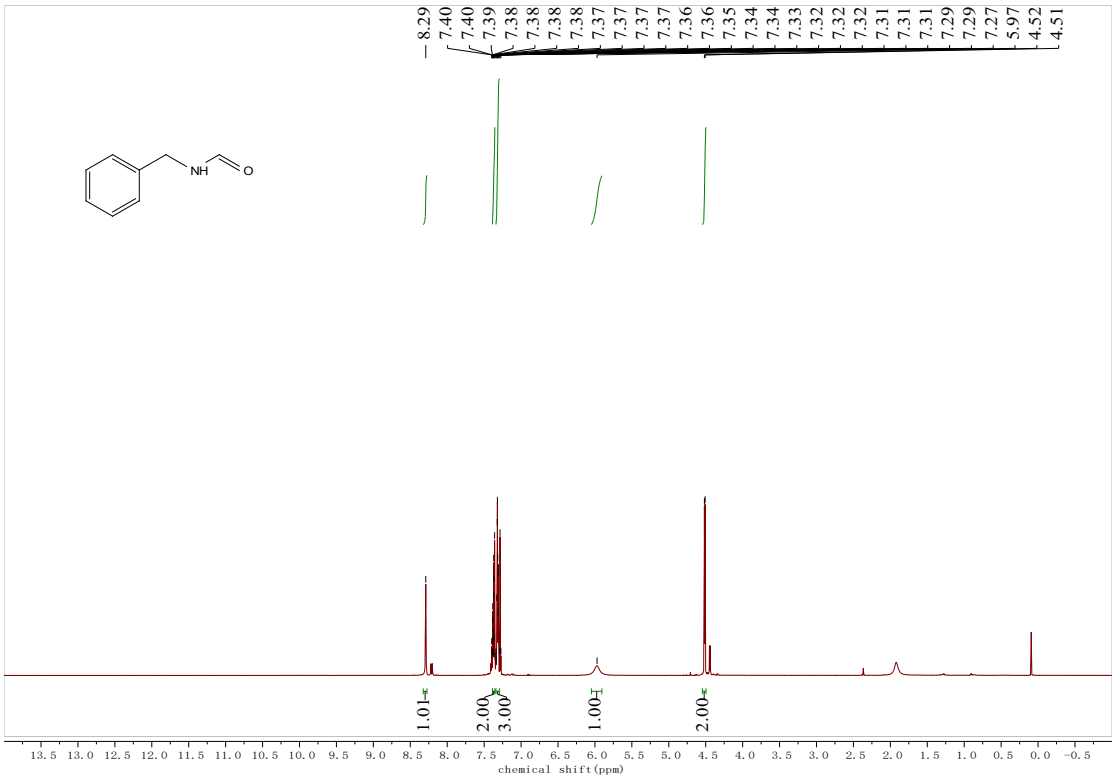


$^{1}$H NMR spectra of **2a**

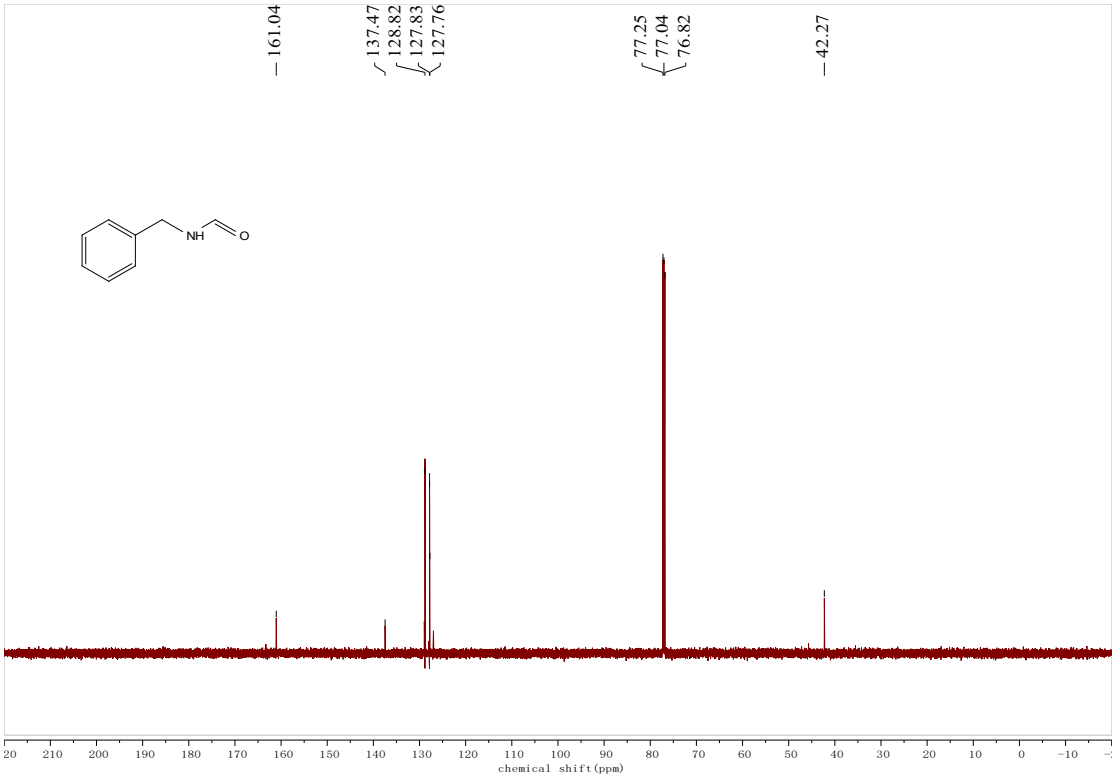


$^{13}$C NMR spectra of **2a**

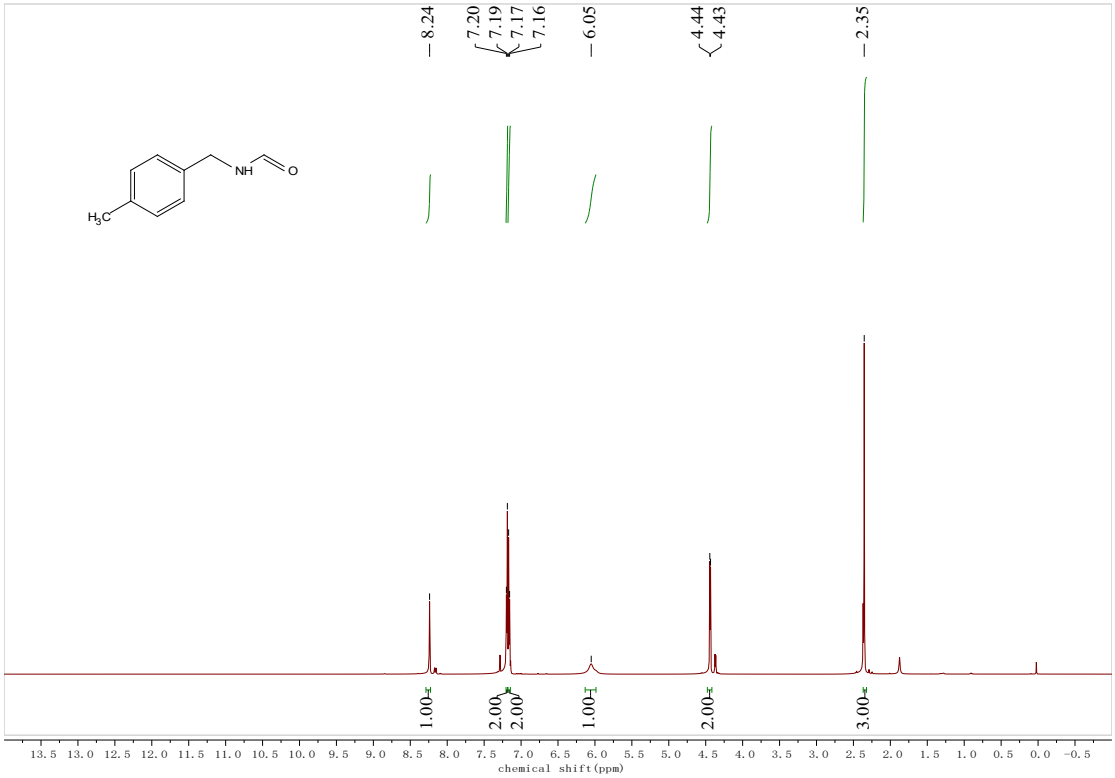


$^{1}$H NMR spectra of **2b**

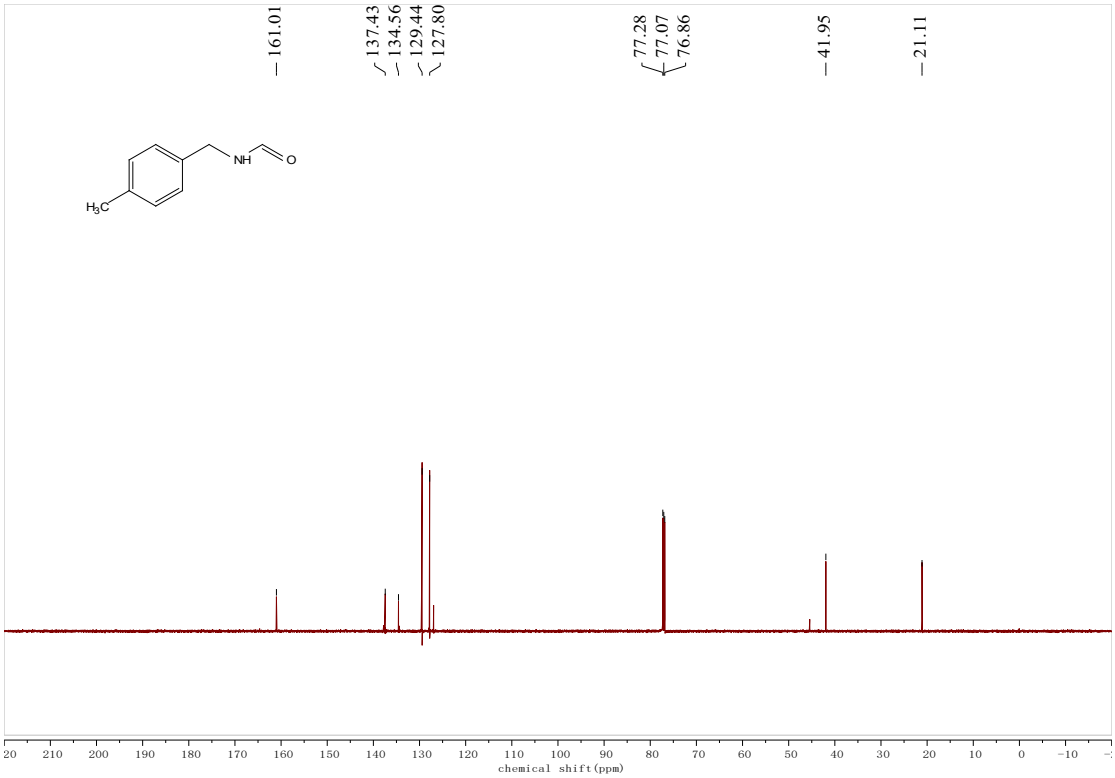


$^{13}$C NMR spectra of **2b**

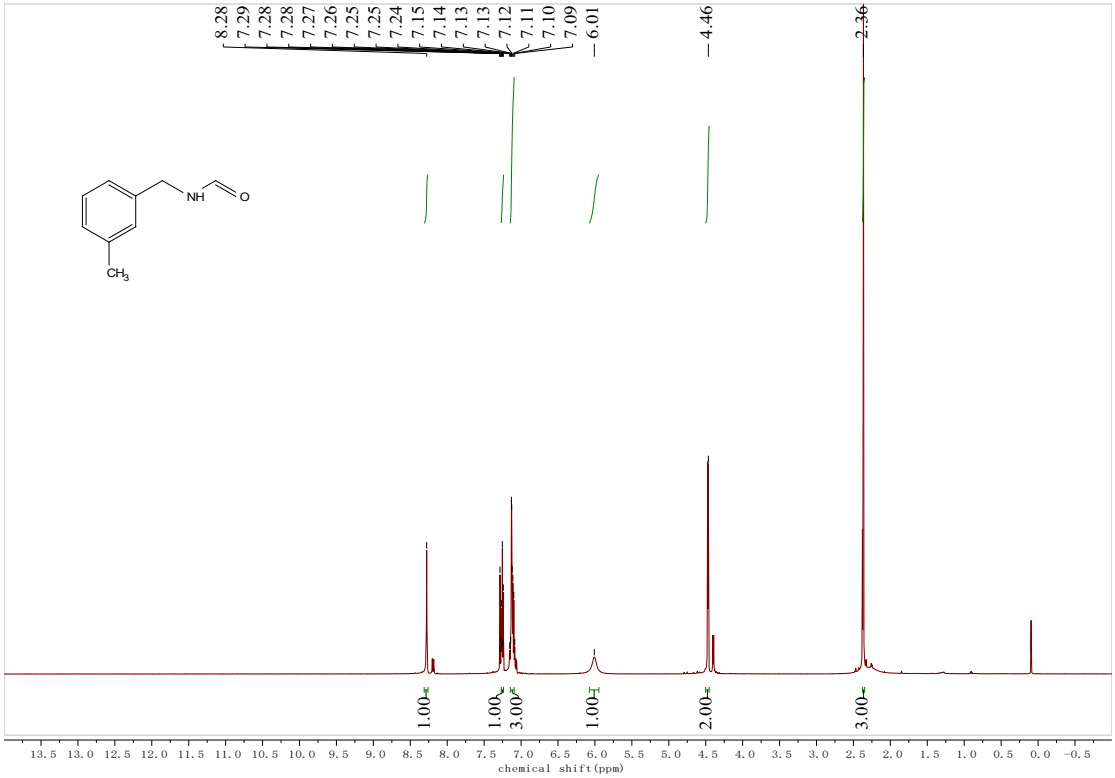


$^{1}$H NMR spectra of **2c**

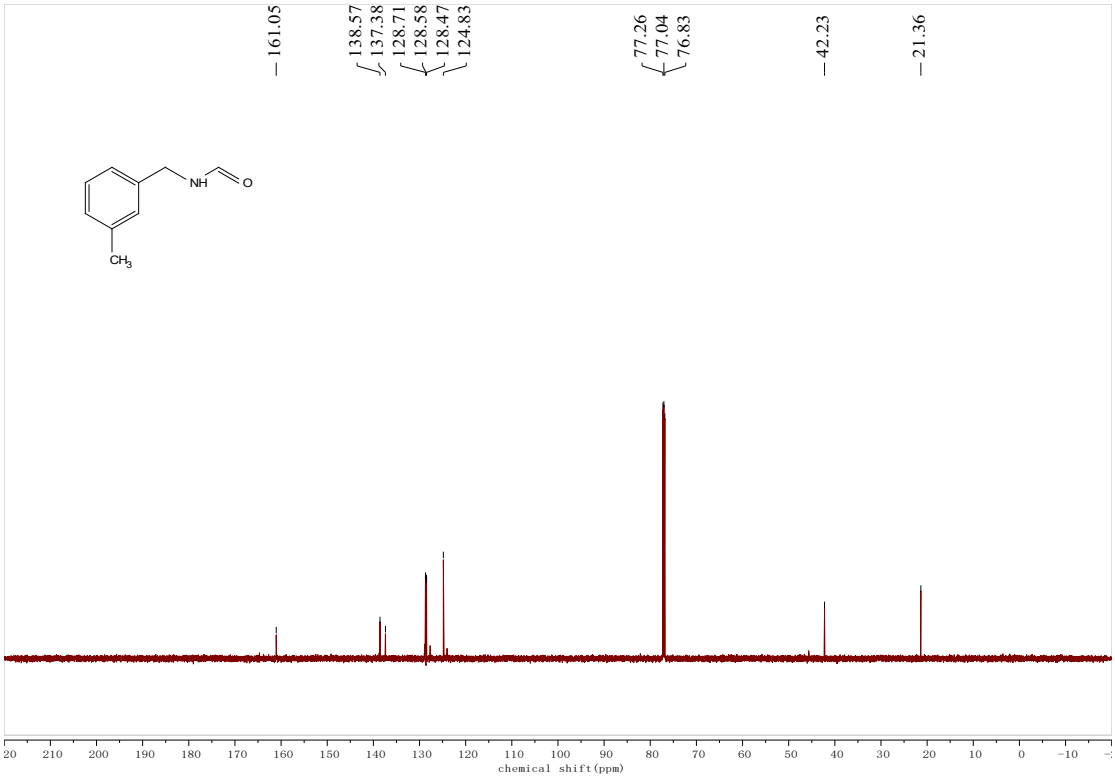


$^{13}$C NMR spectra of **2c**

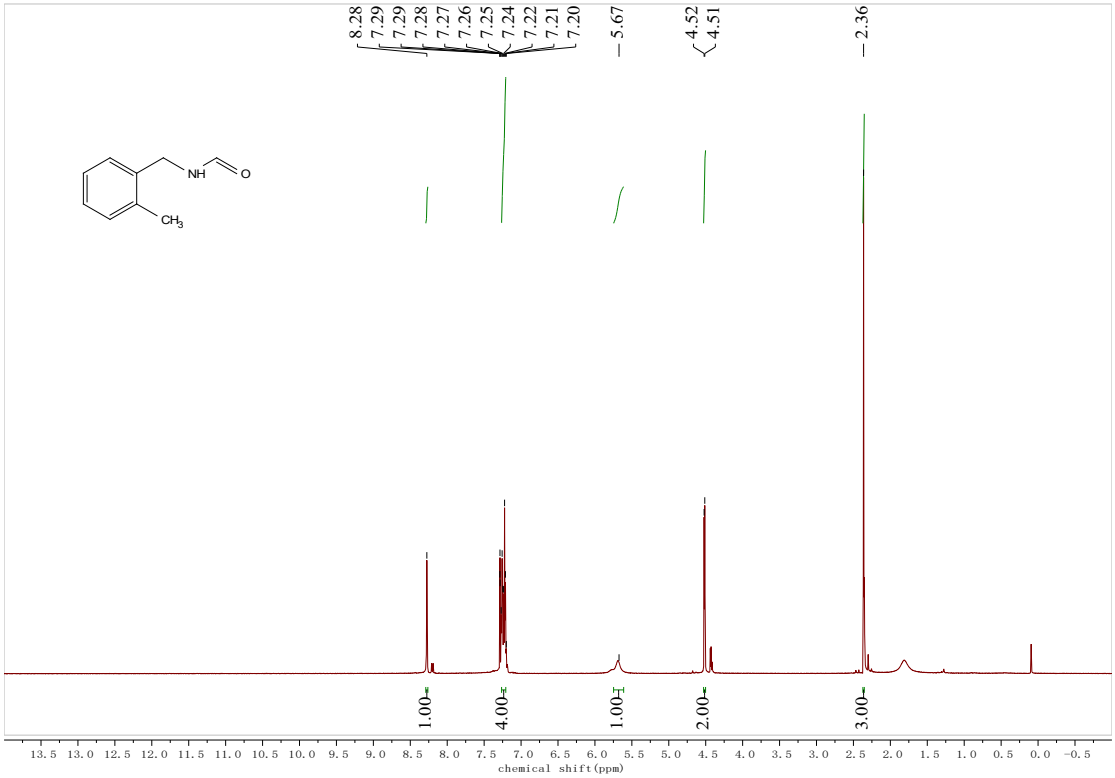


$^{1}$H NMR spectra of **2d**

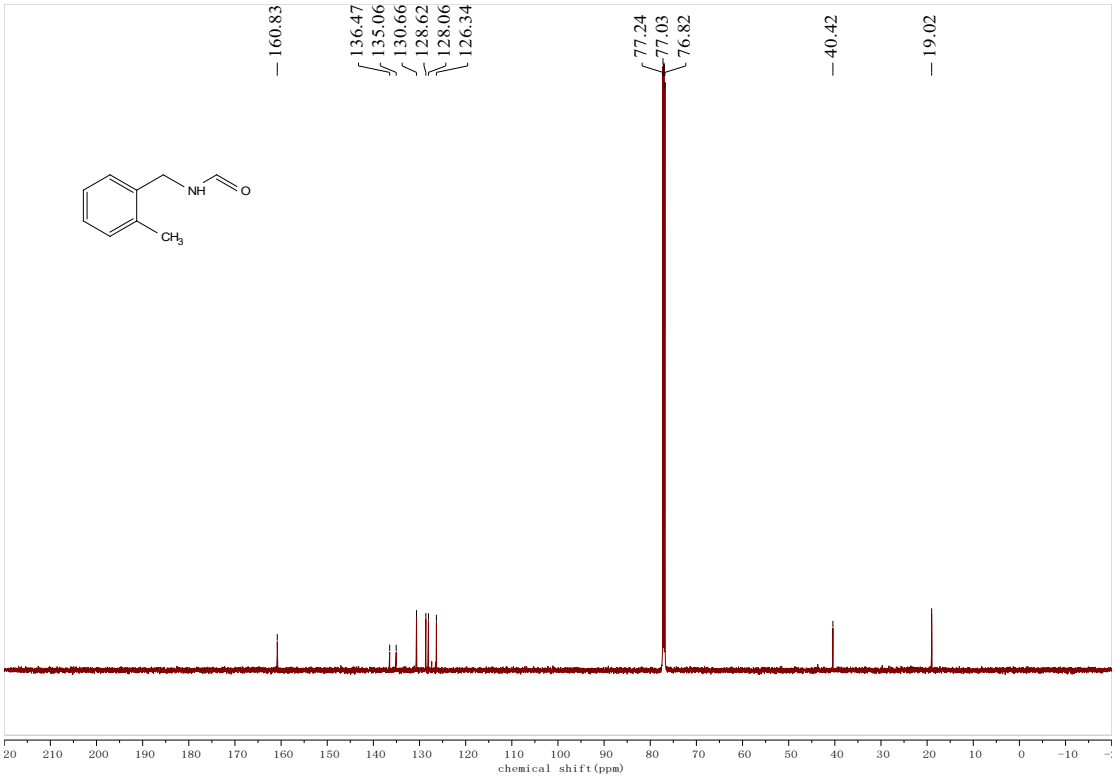


$^{13}$C NMR spectra of **2d**

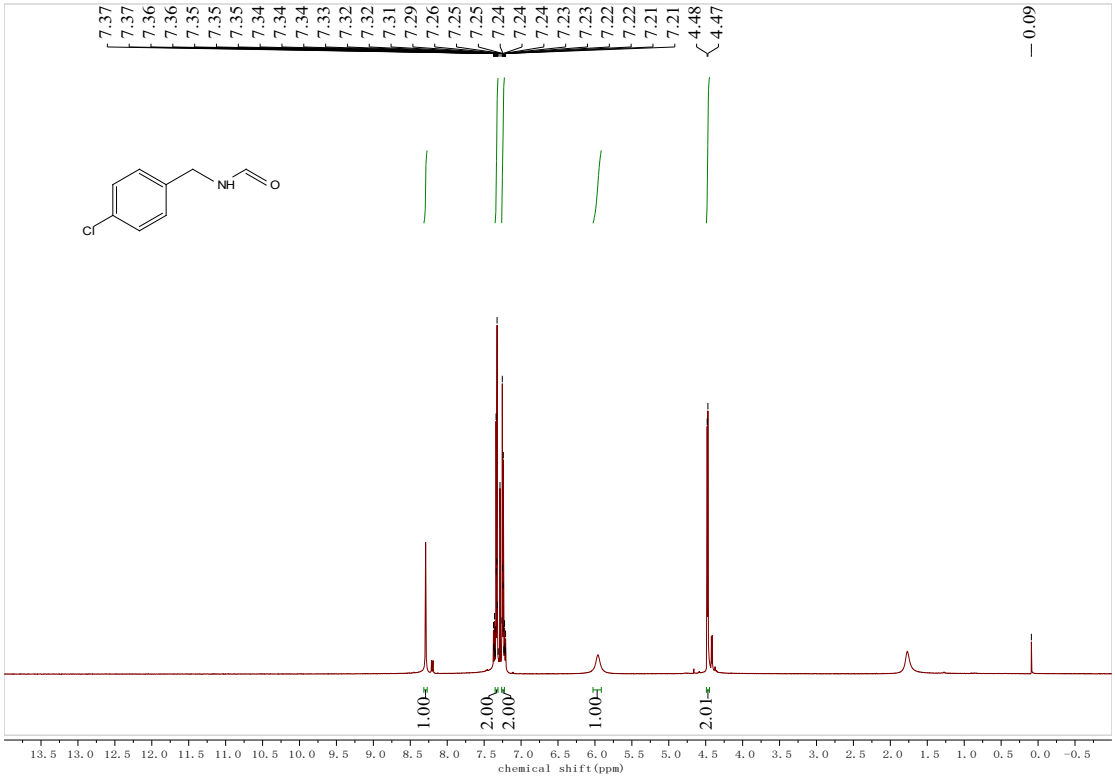


$^{1}$H NMR spectra of **2e**

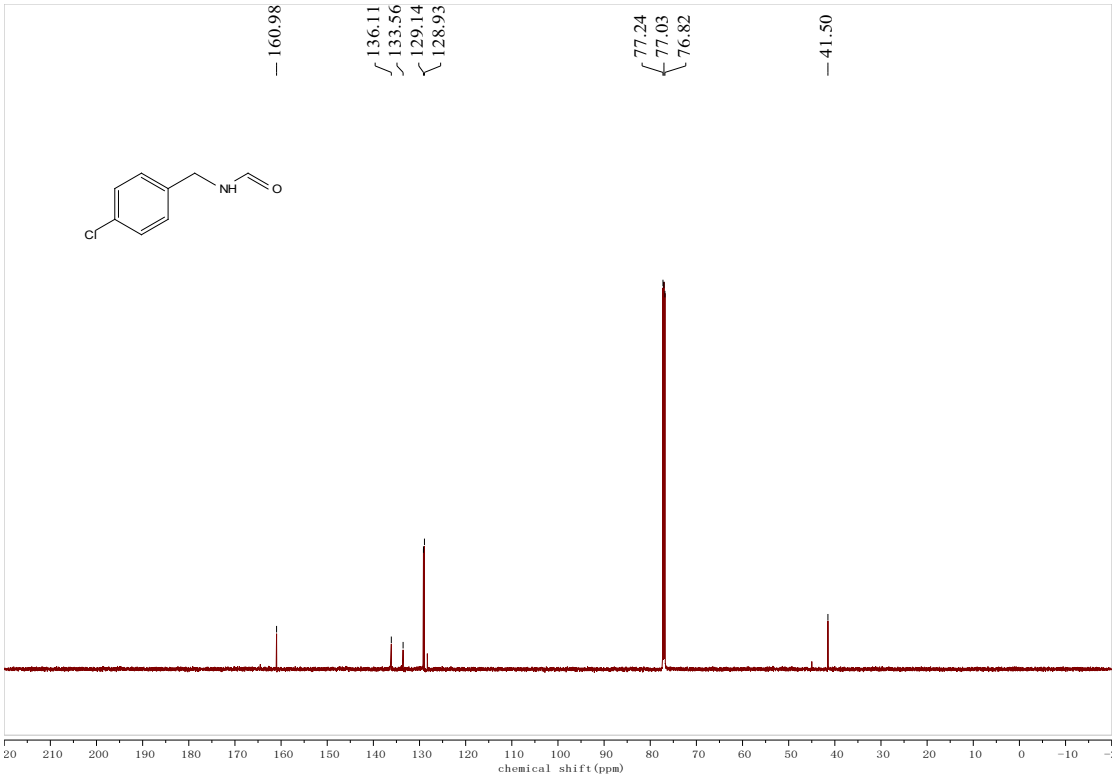


$^{13}$C NMR spectra of **2e**

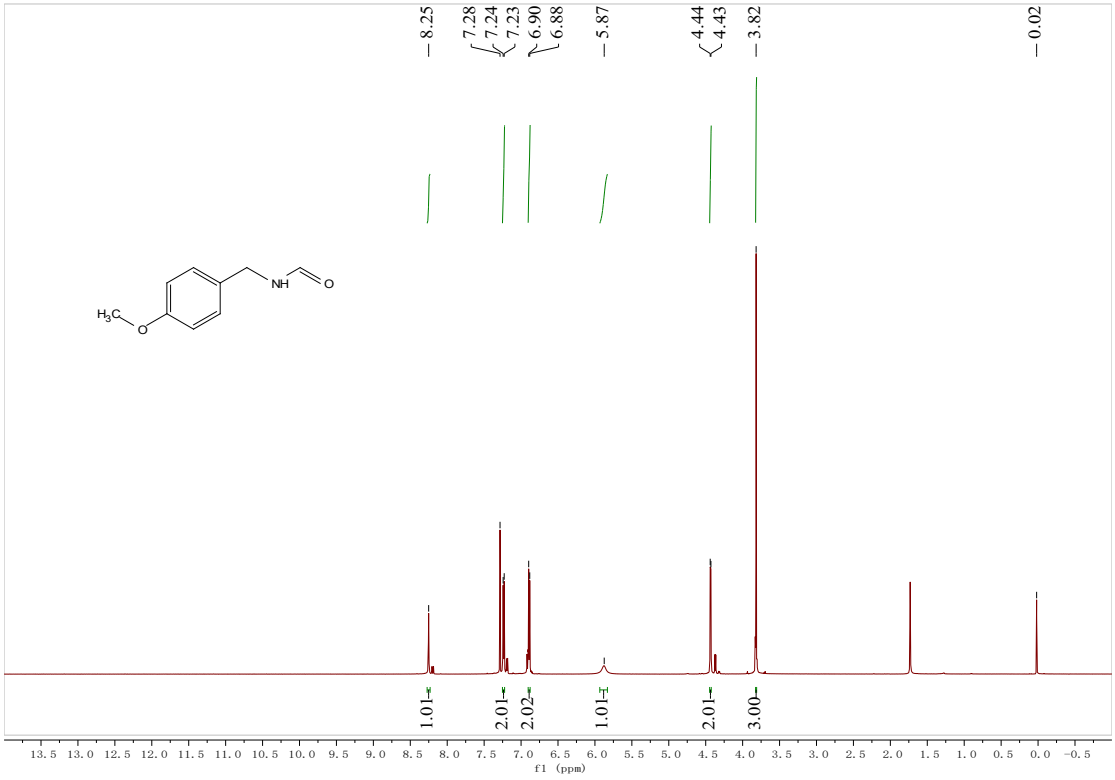


$^{1}$H NMR spectra of **2f**

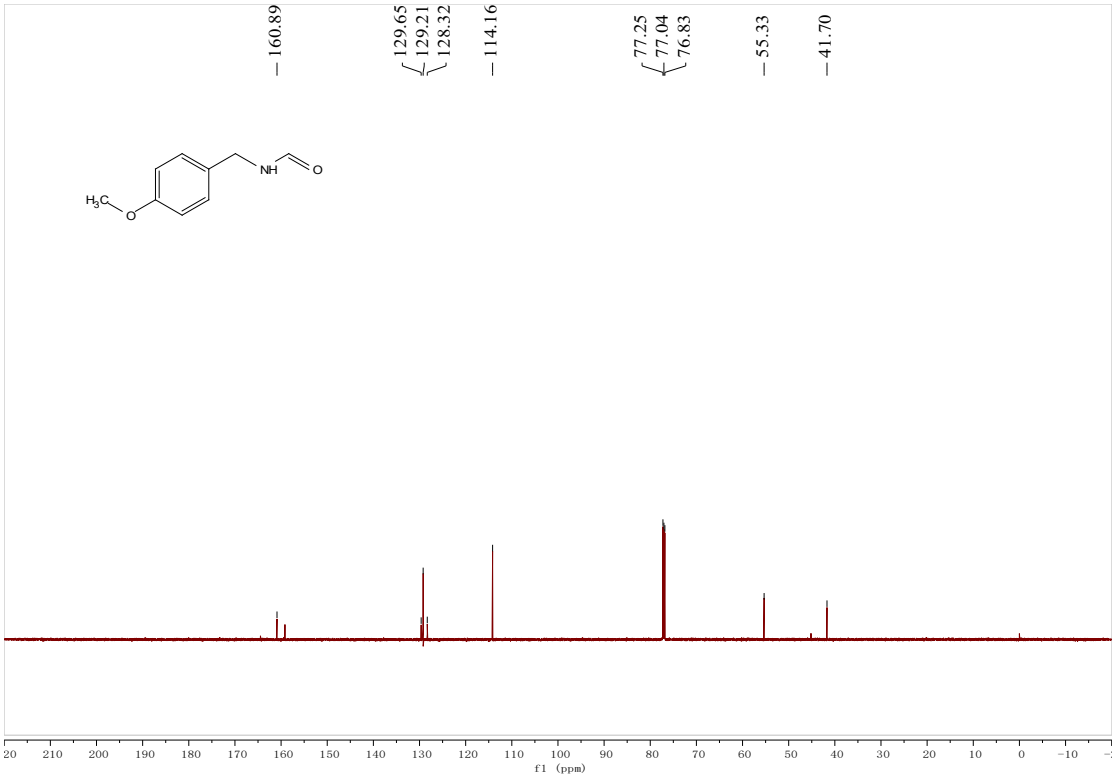


$^{13}$C NMR spectra of **2f**

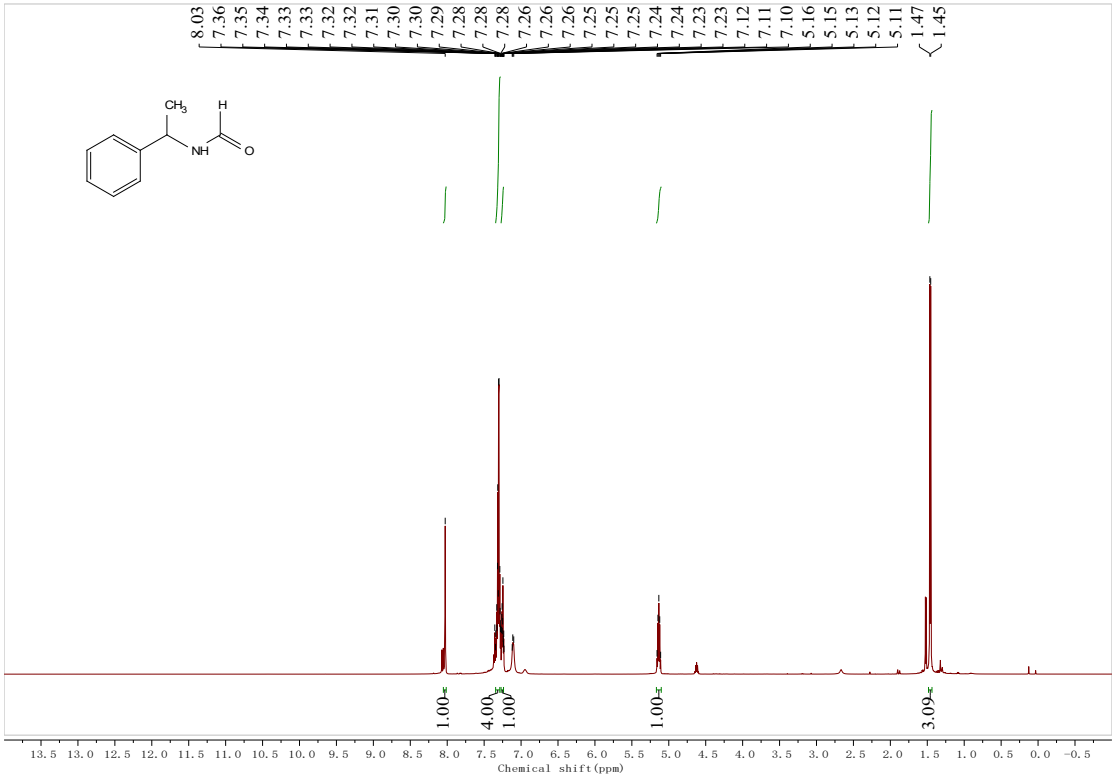


$^{1}$H NMR spectra of **2g**

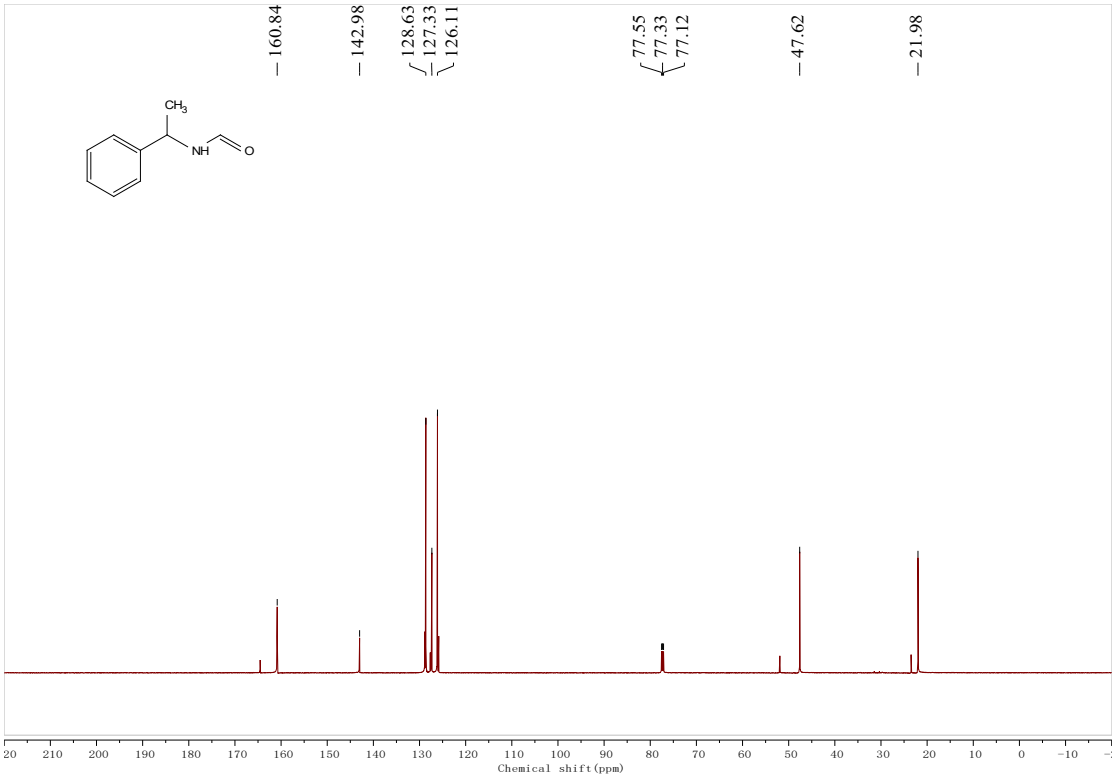


$^{13}$C NMR spectra of **2g**

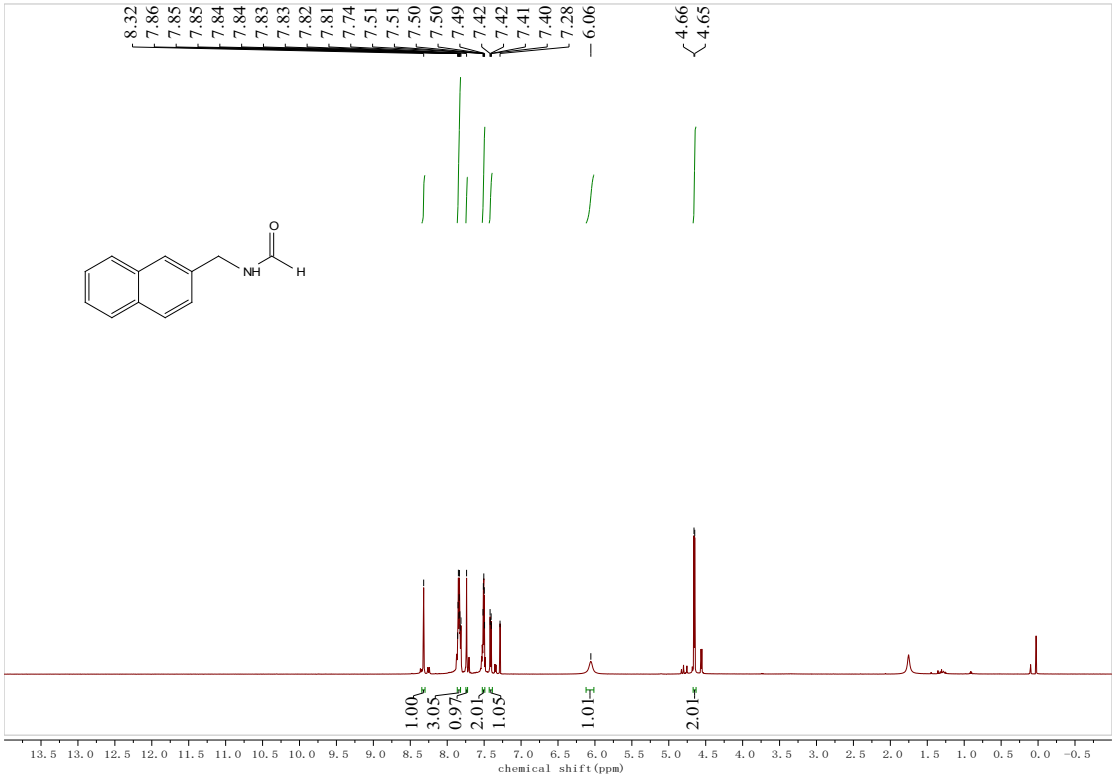


$^{1}$H NMR spectra of **2h**

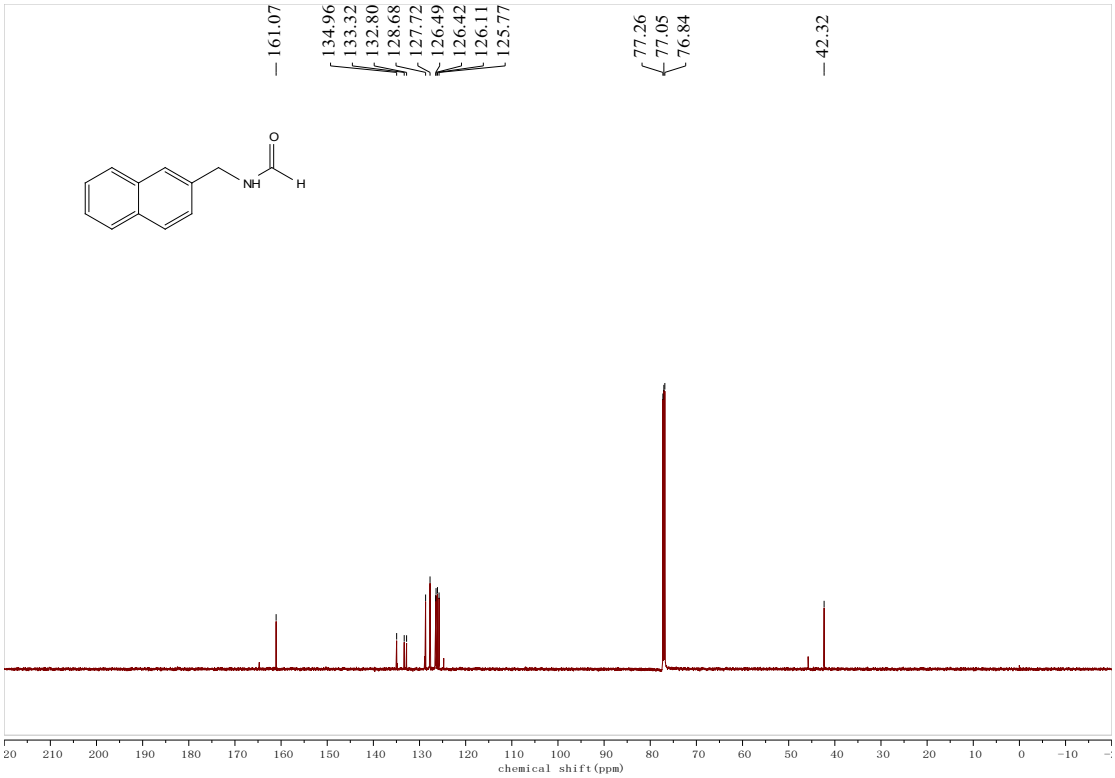


$^{13}$C NMR spectra of **2h**

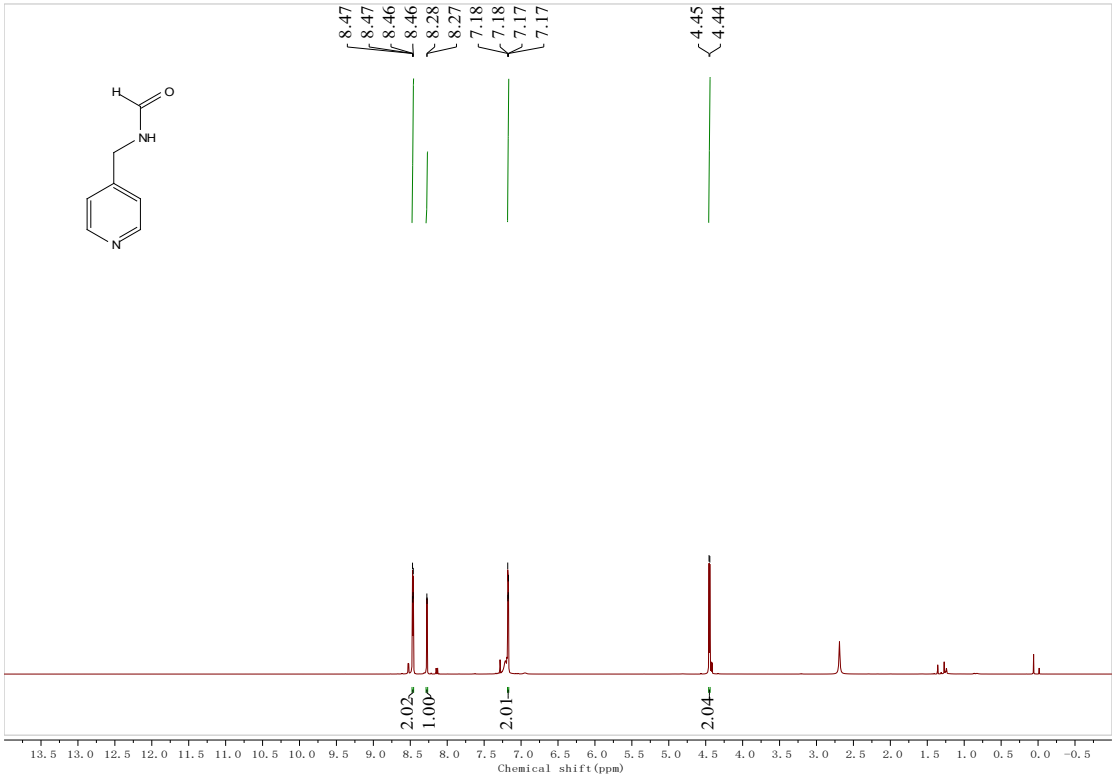


$^{1}$H NMR spectra of **2i**

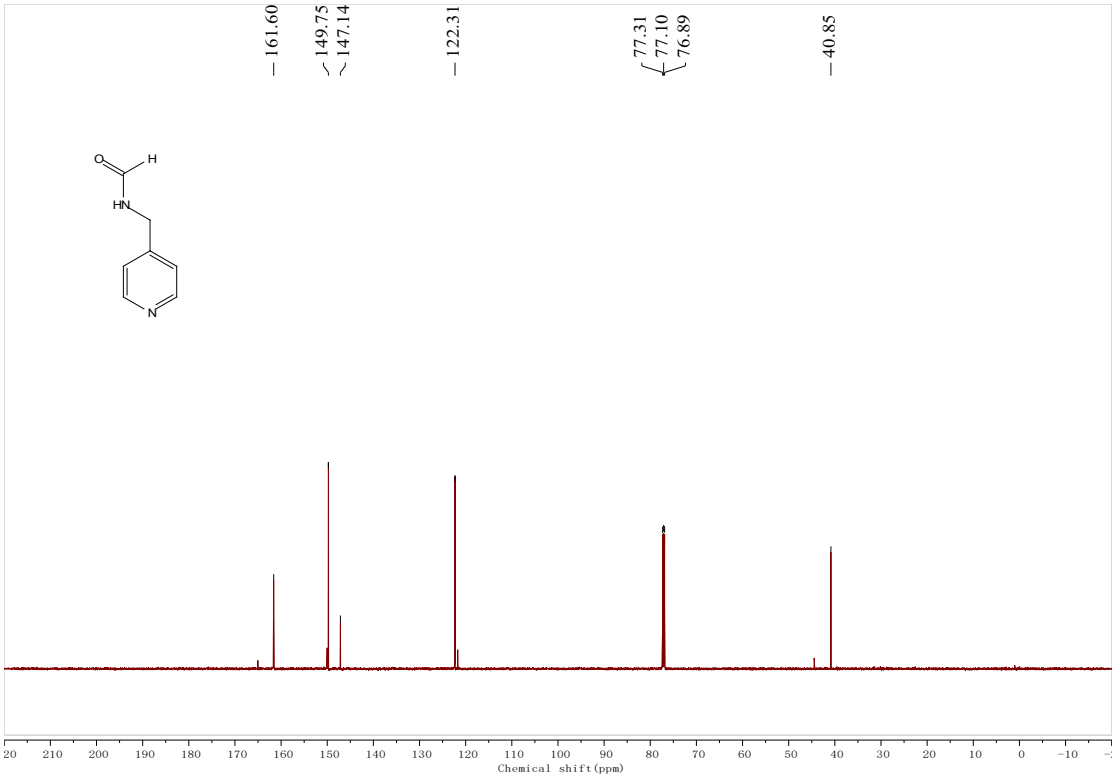


$^{13}$C NMR spectra of **2i**

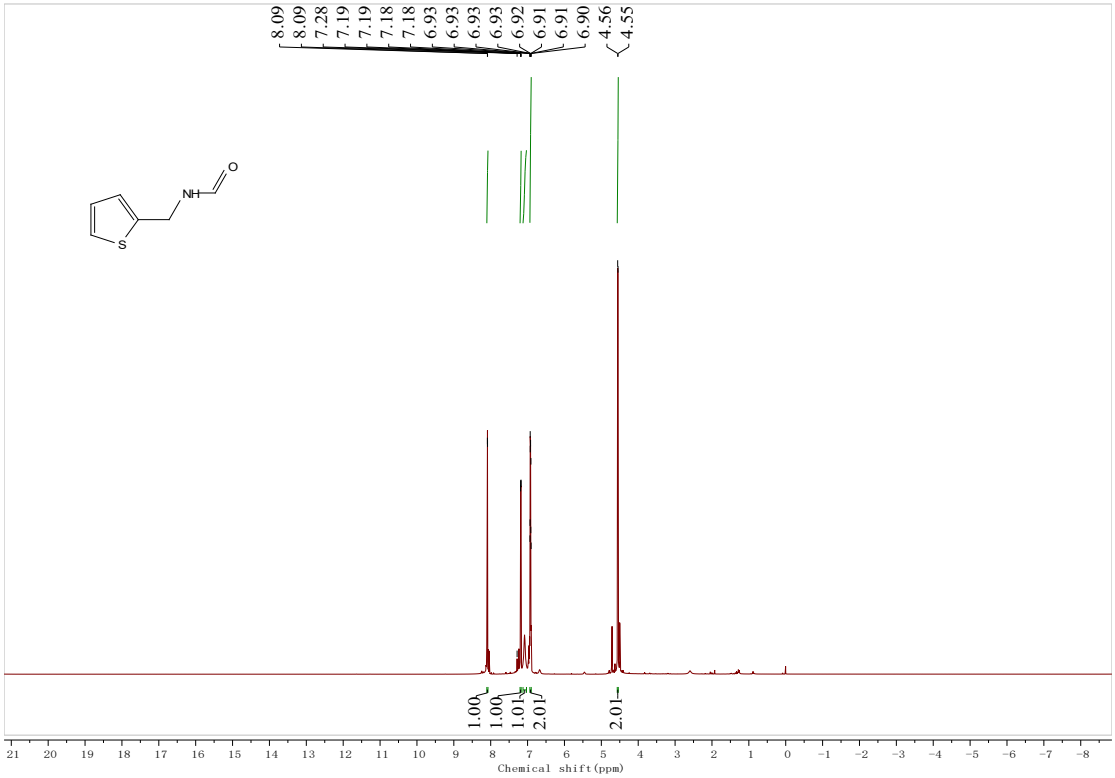


$^{1}$H NMR spectra of **2j**

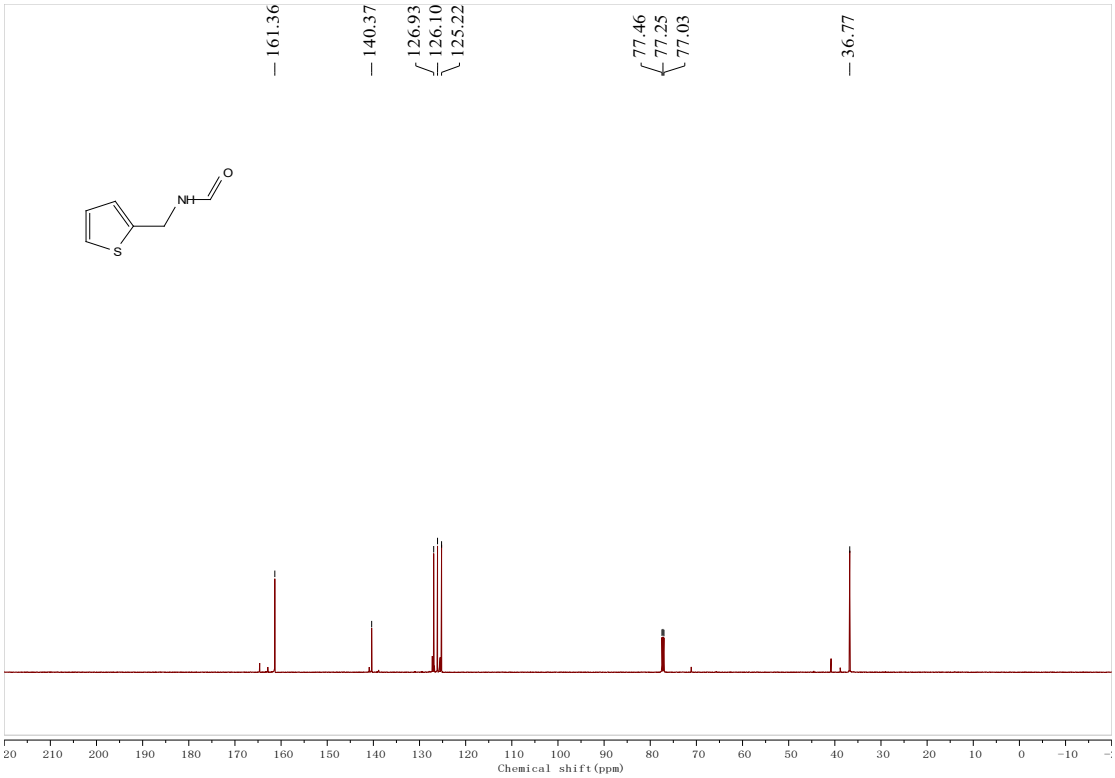


$^{13}$C NMR spectra of **2j**

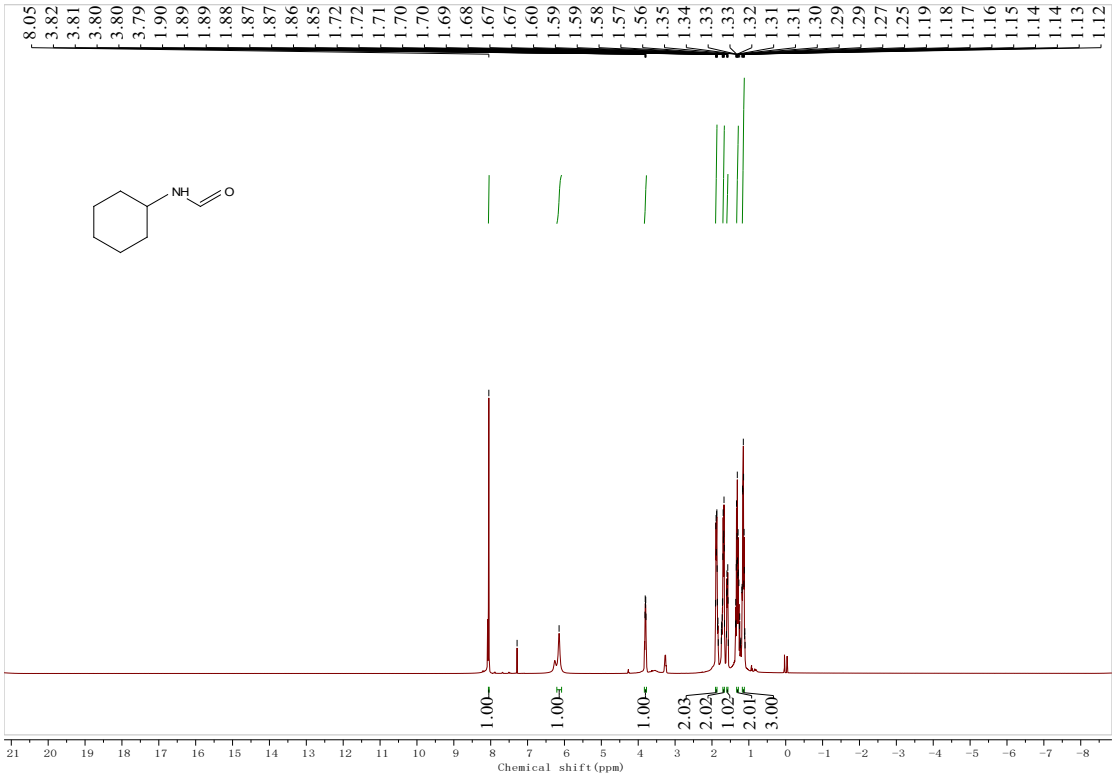


$^{1}$H NMR spectra of **2k**

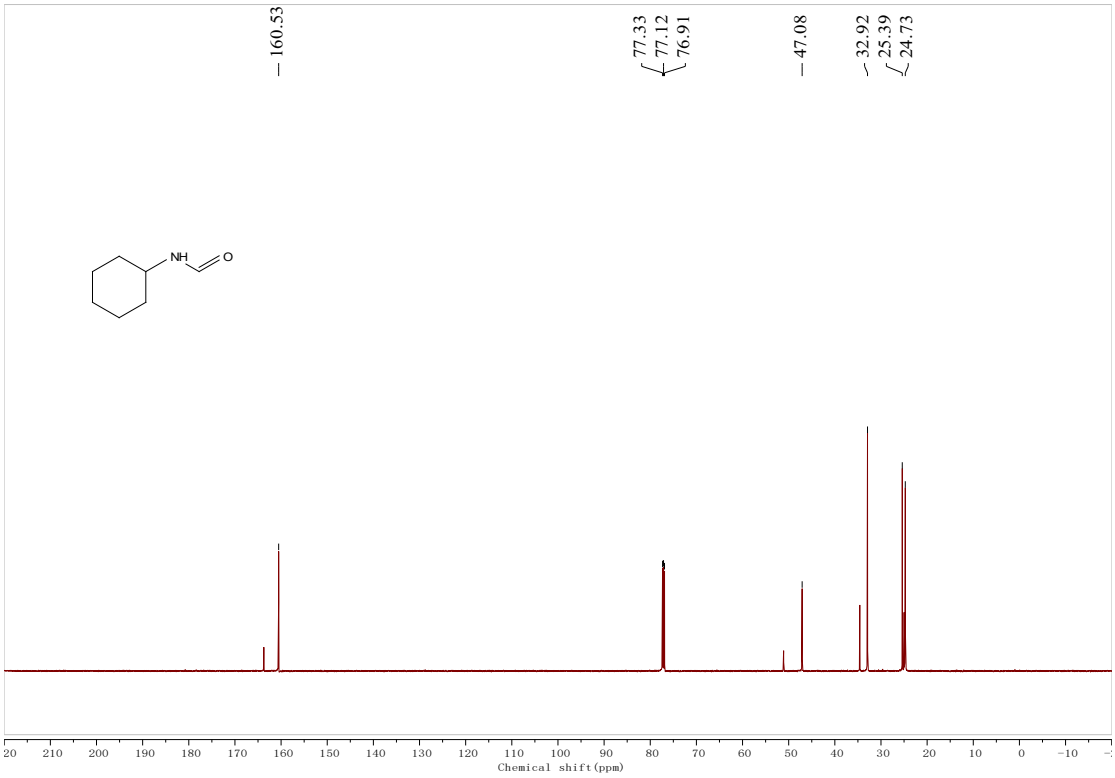


$^{13}$C NMR spectra of **2k**

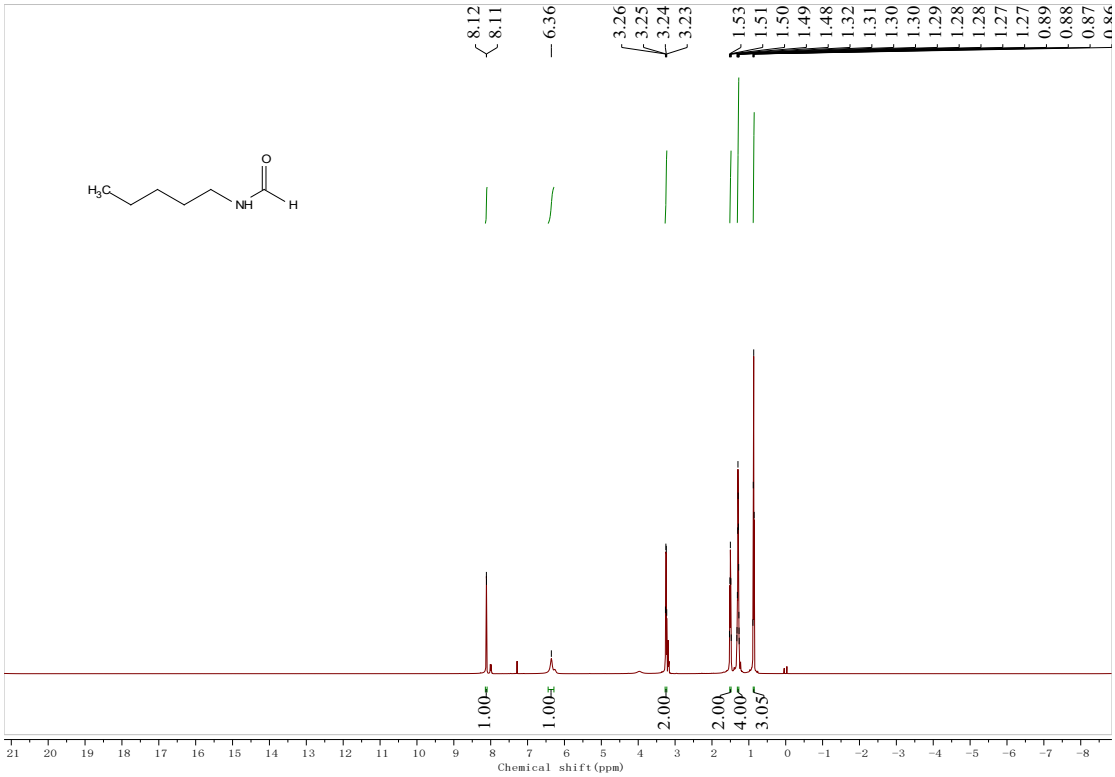


$^{1}$H NMR spectra of **2l**

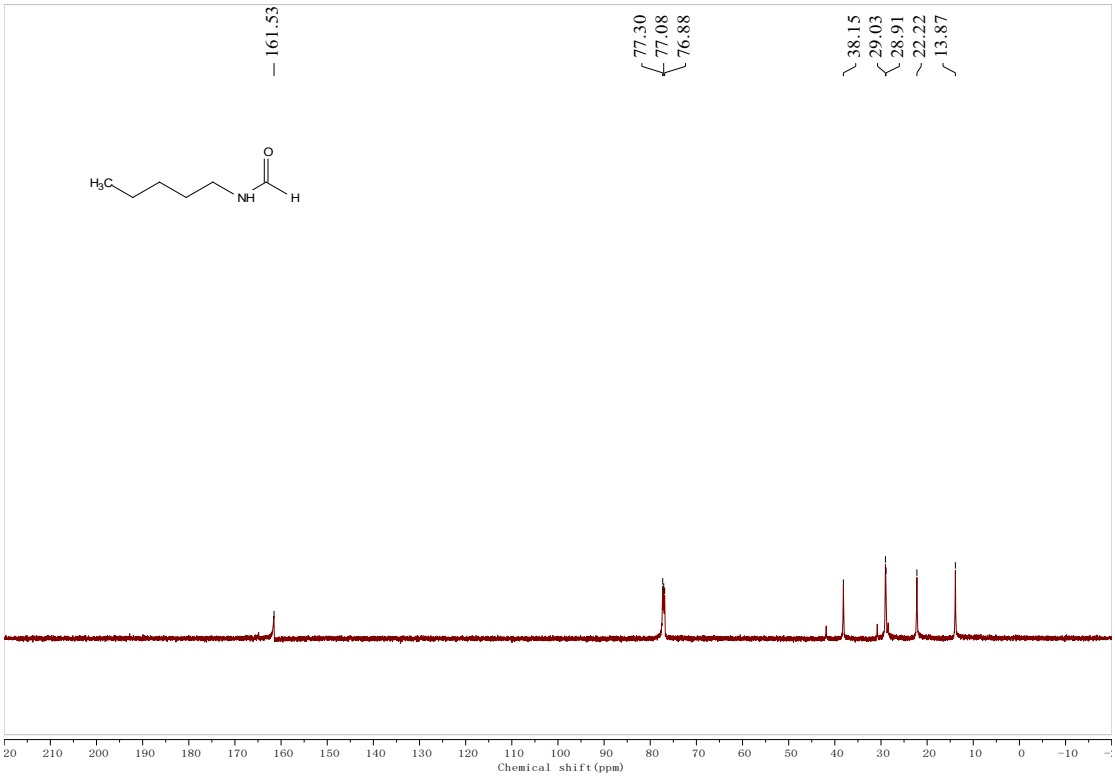


$^{13}$C NMR spectra of **2l**

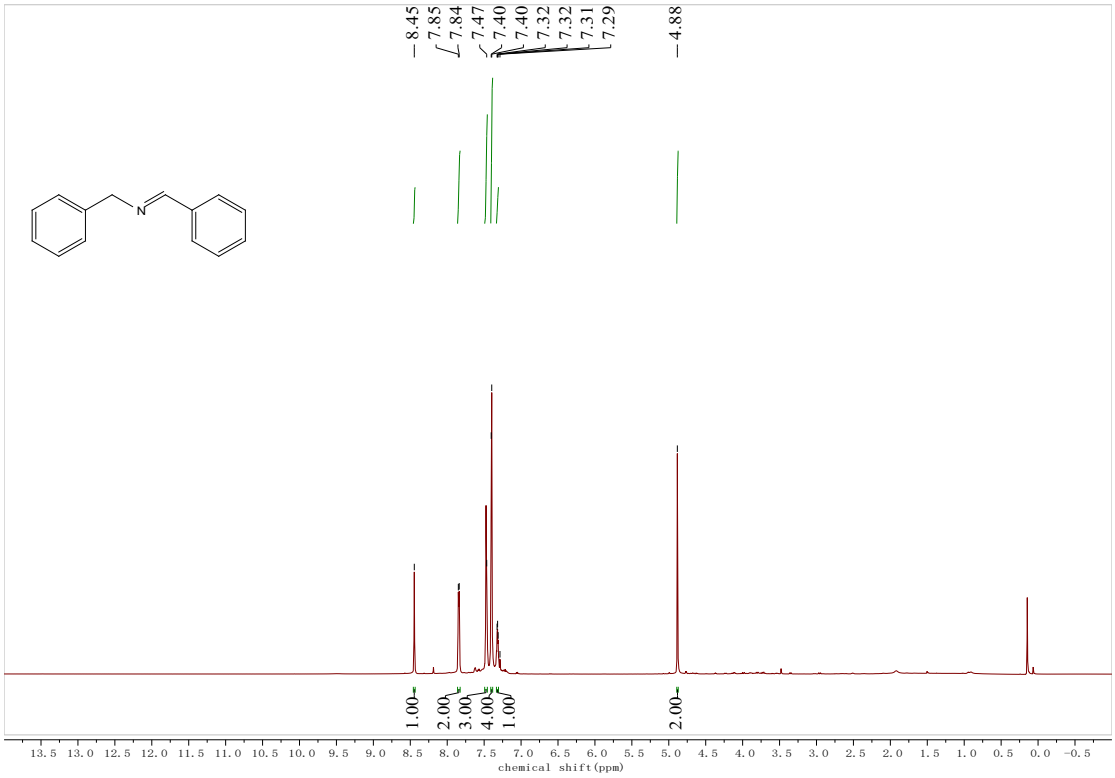


$^{1}$H NMR spectra of **4a**

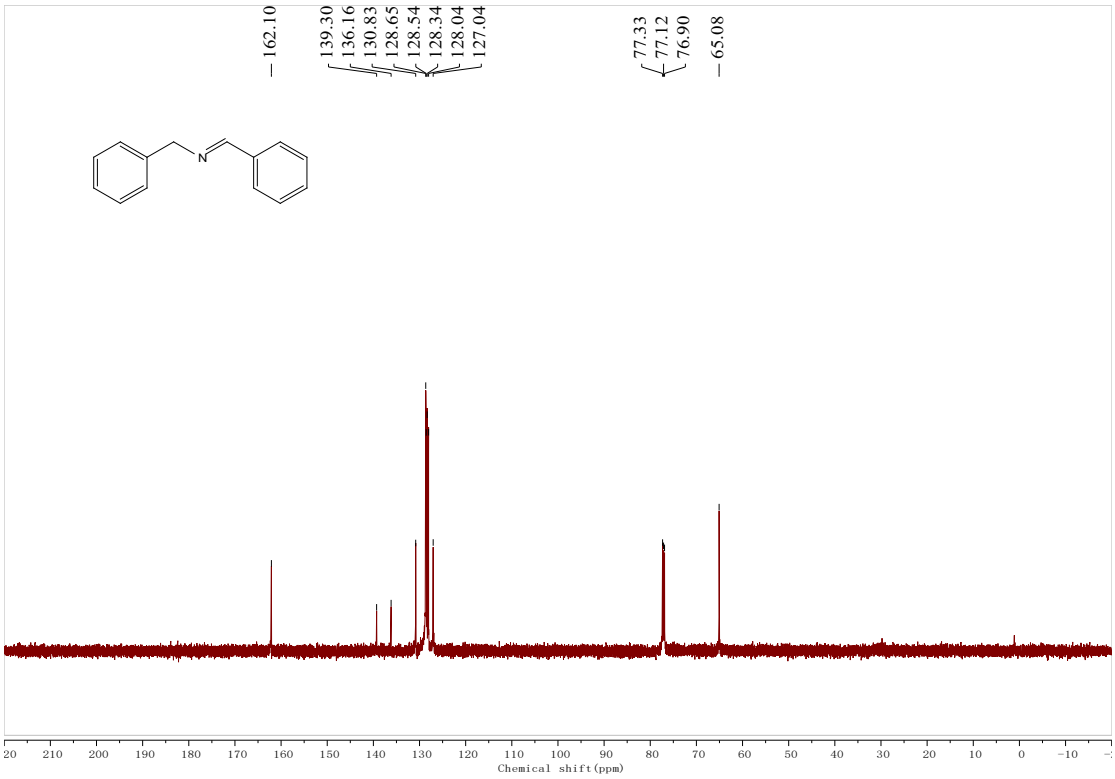


$^{13}$C NMR spectra of **4a**

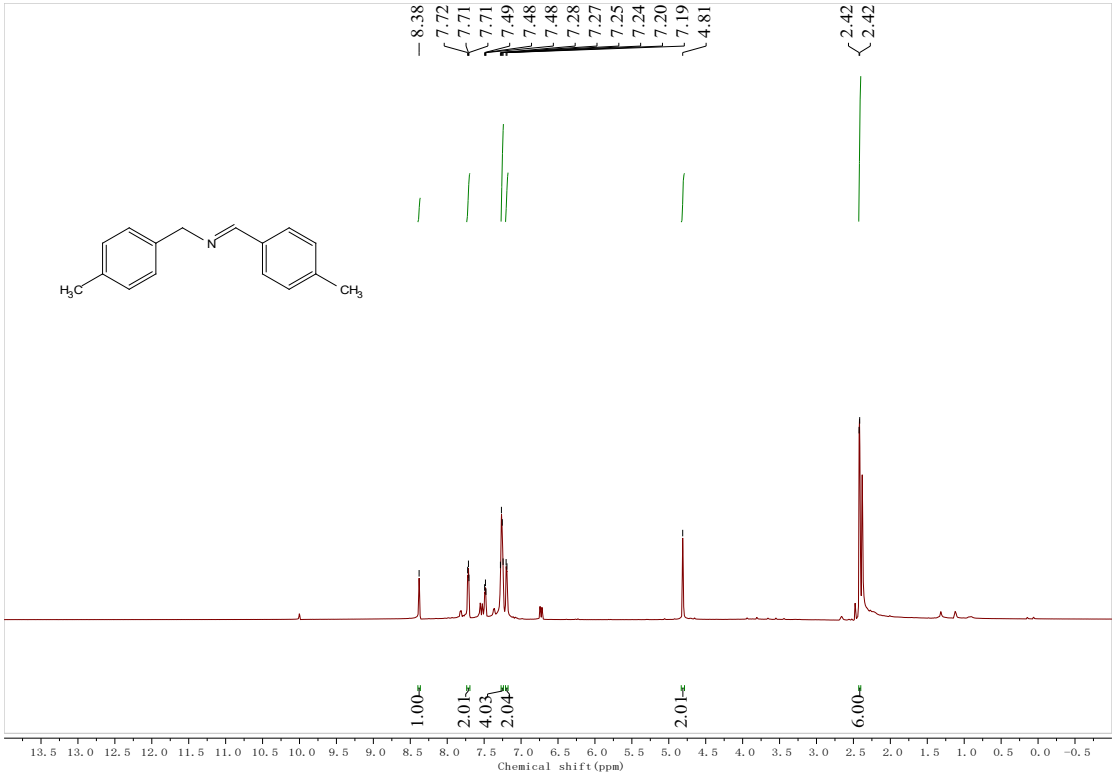


$^{1}$H NMR spectra of **4b**

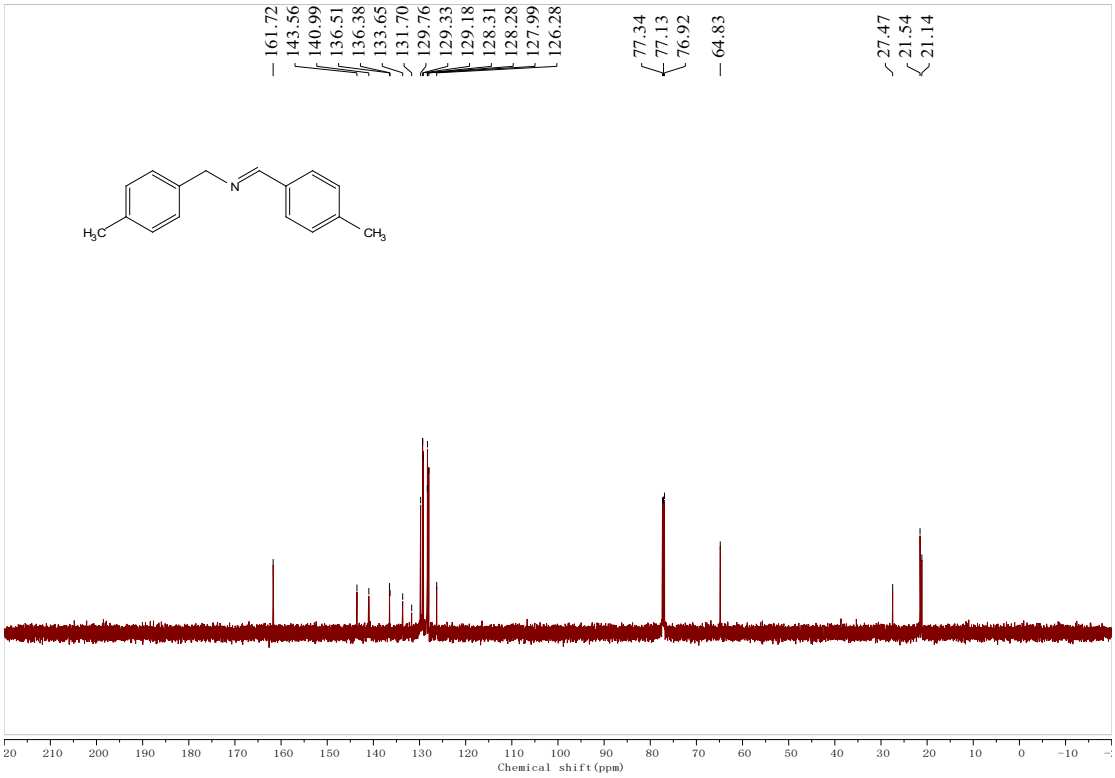


$^{13}$C NMR spectra of **4b**

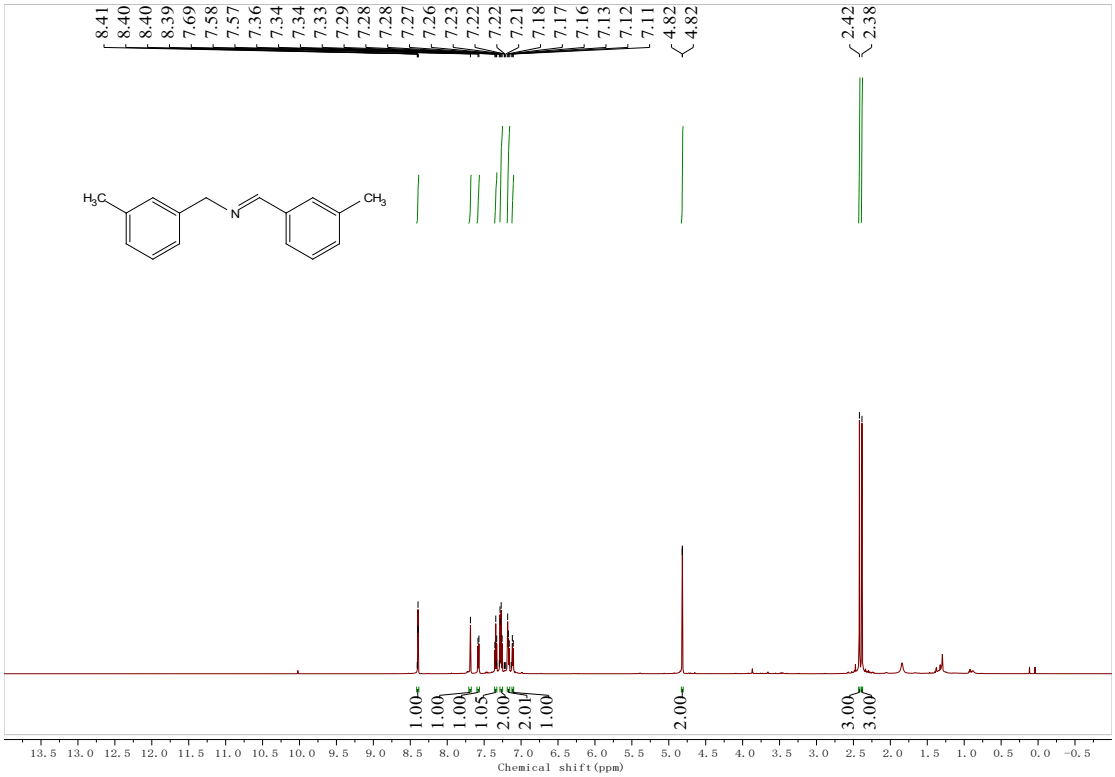


$^{1}$H NMR spectra of **4c**

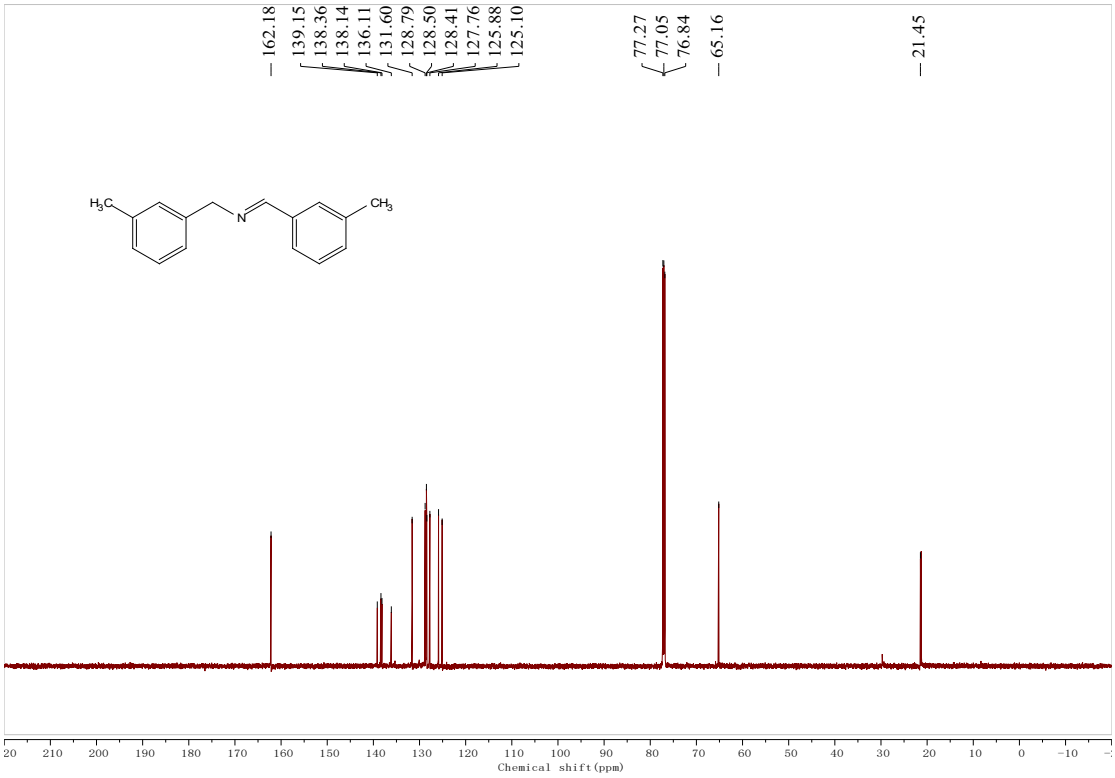


$^{13}$C NMR spectra of **4c**

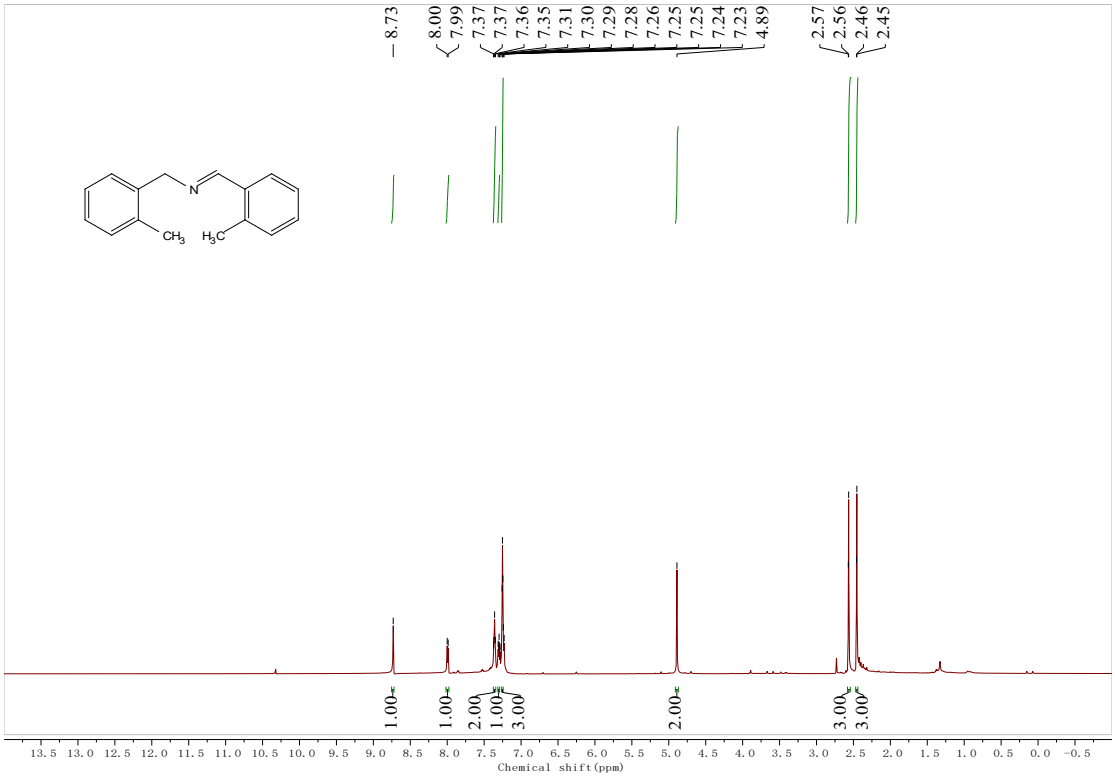


$^{1}$H NMR spectra of **4d**

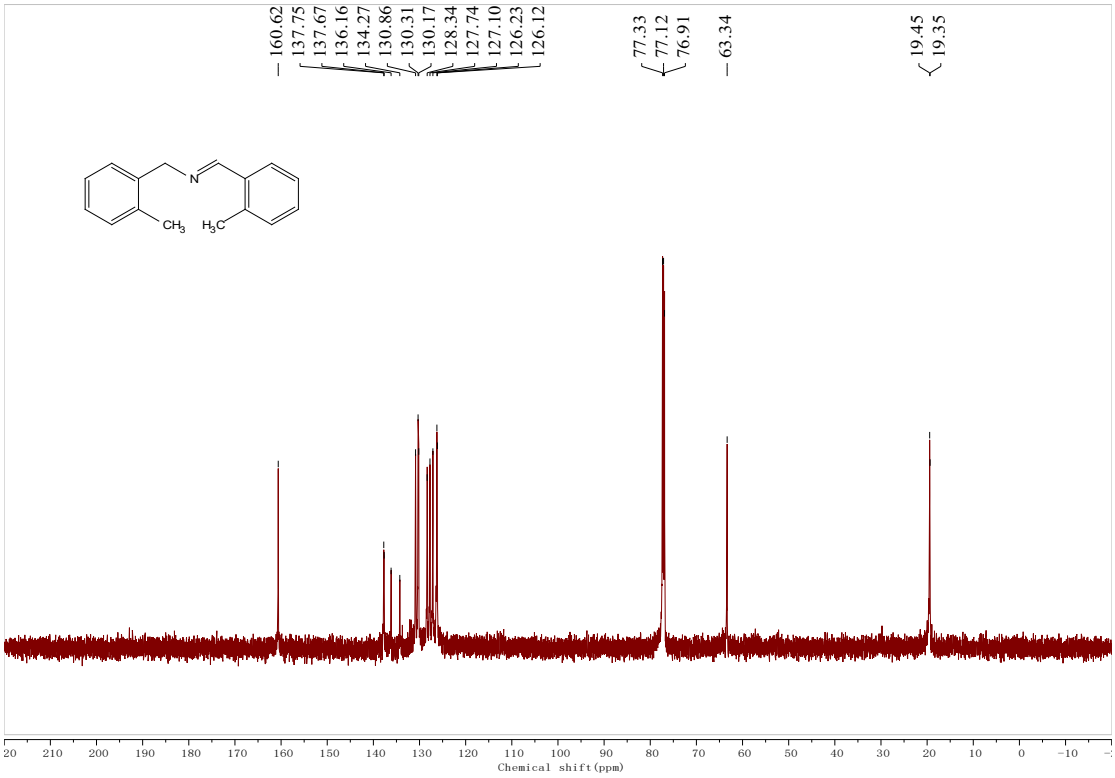


$^{13}$C NMR spectra of **4d**

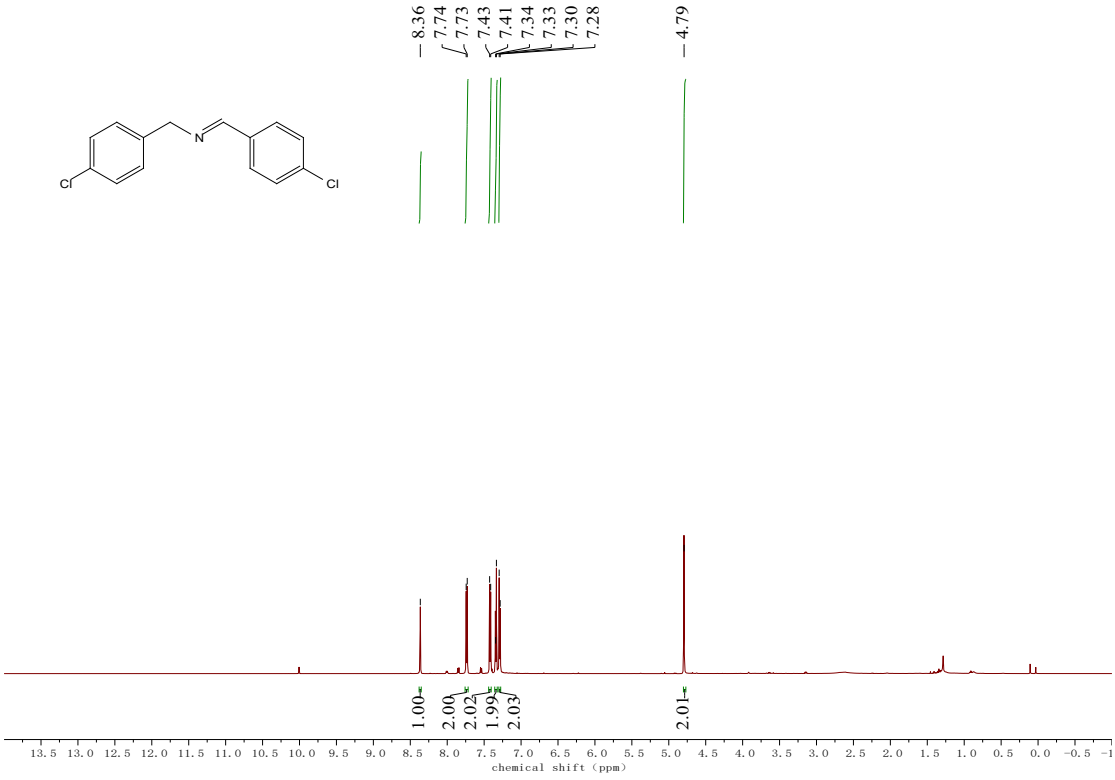


$^{1}$H NMR spectra of **4e**

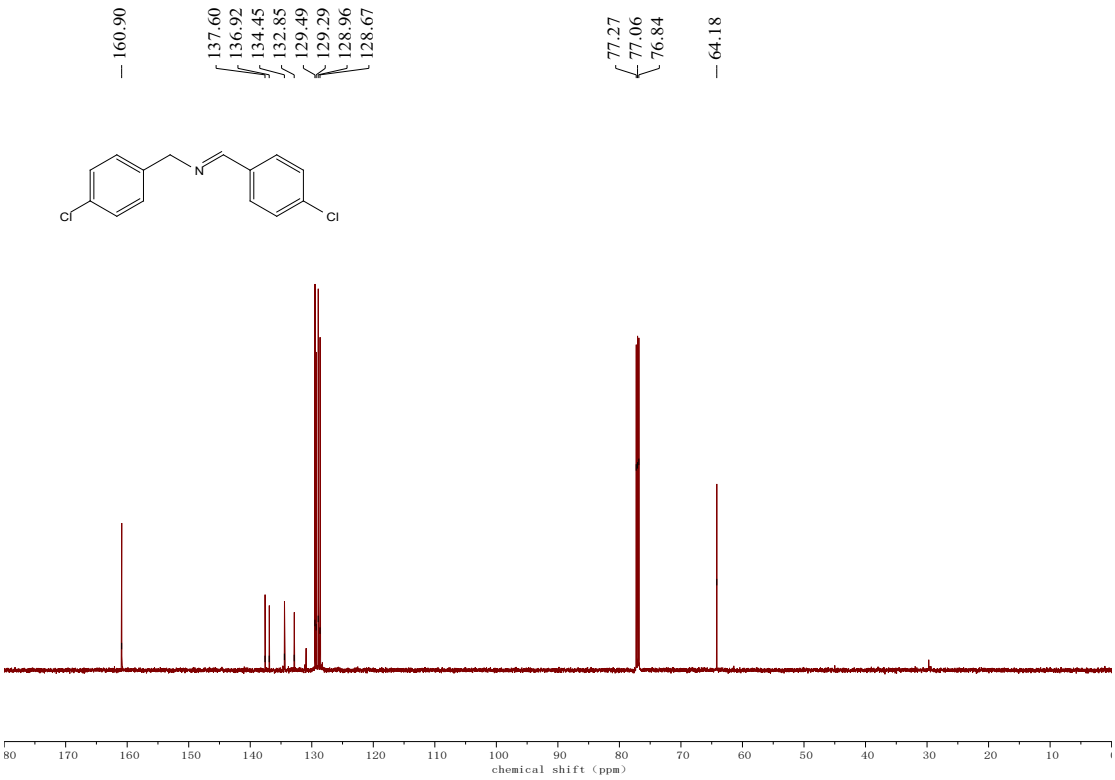


$^{13}$C NMR spectra of **4e**

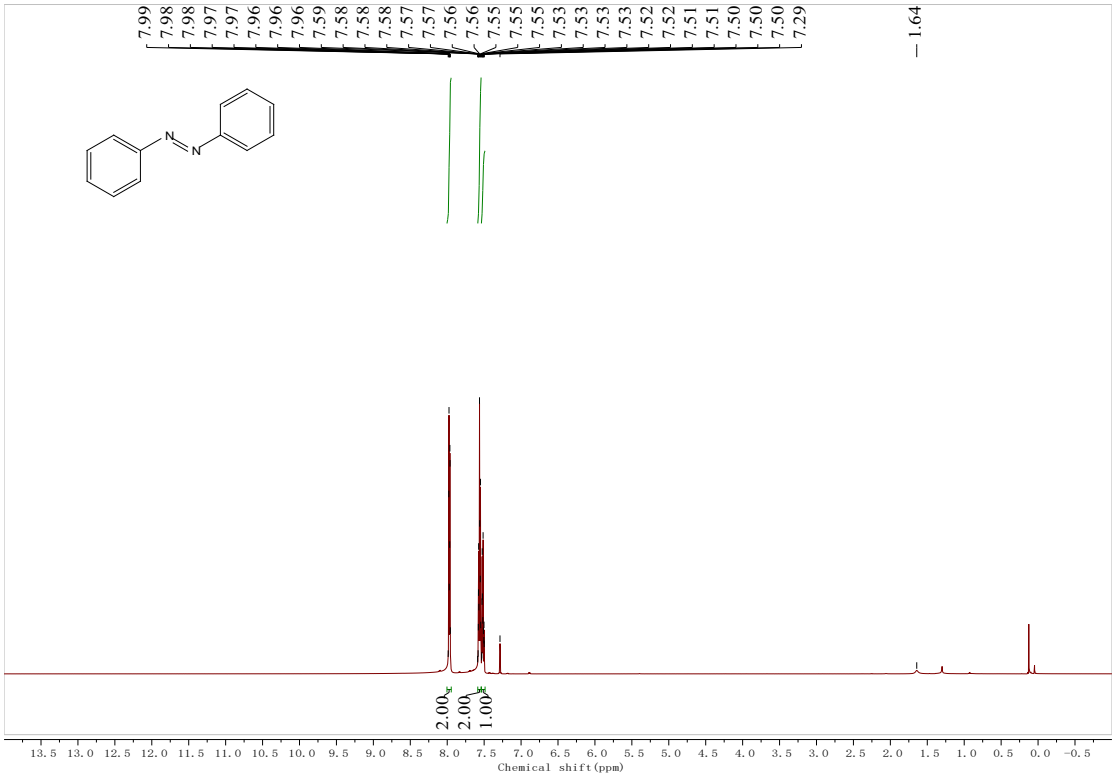


$^{1}$H NMR spectra of **6a**

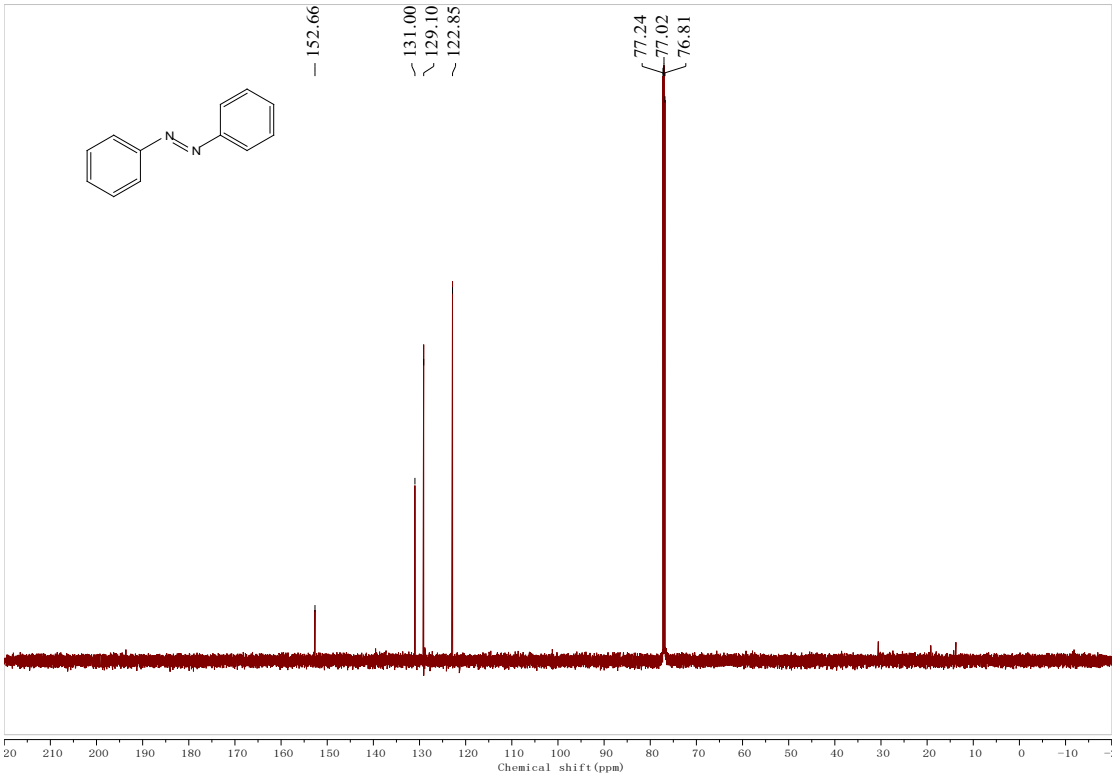


$^{13}$C NMR spectra of **6a**

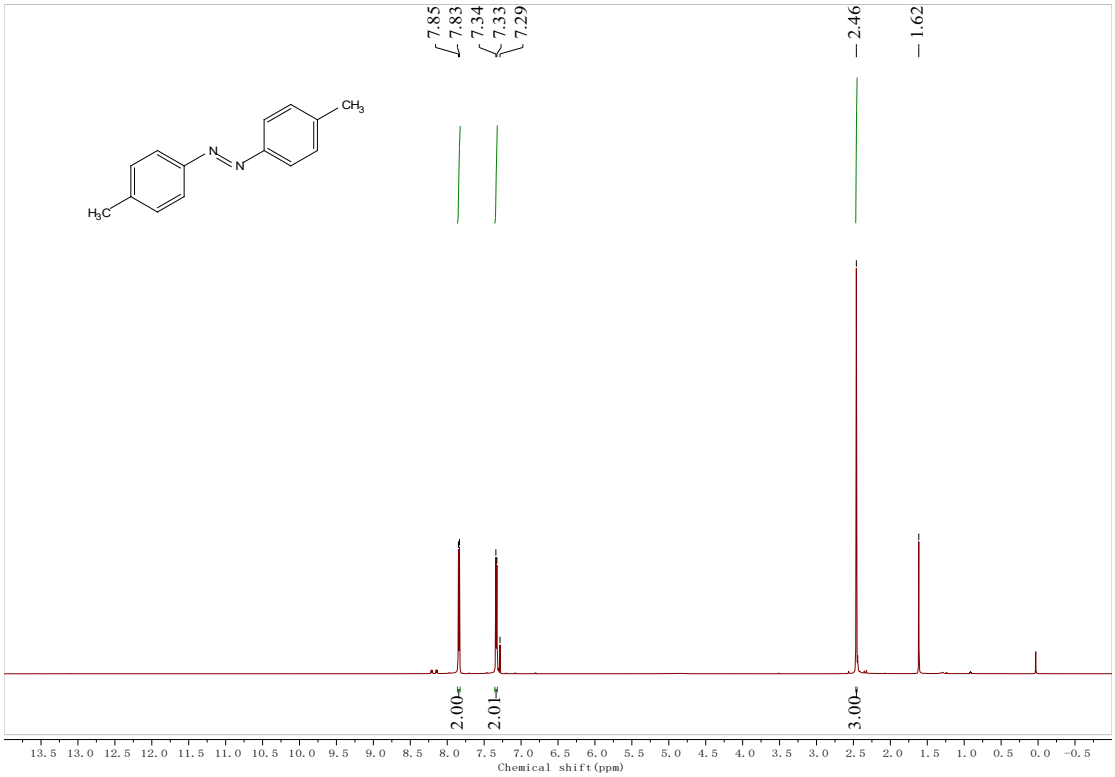


$^{1}$H NMR spectra of **6b**

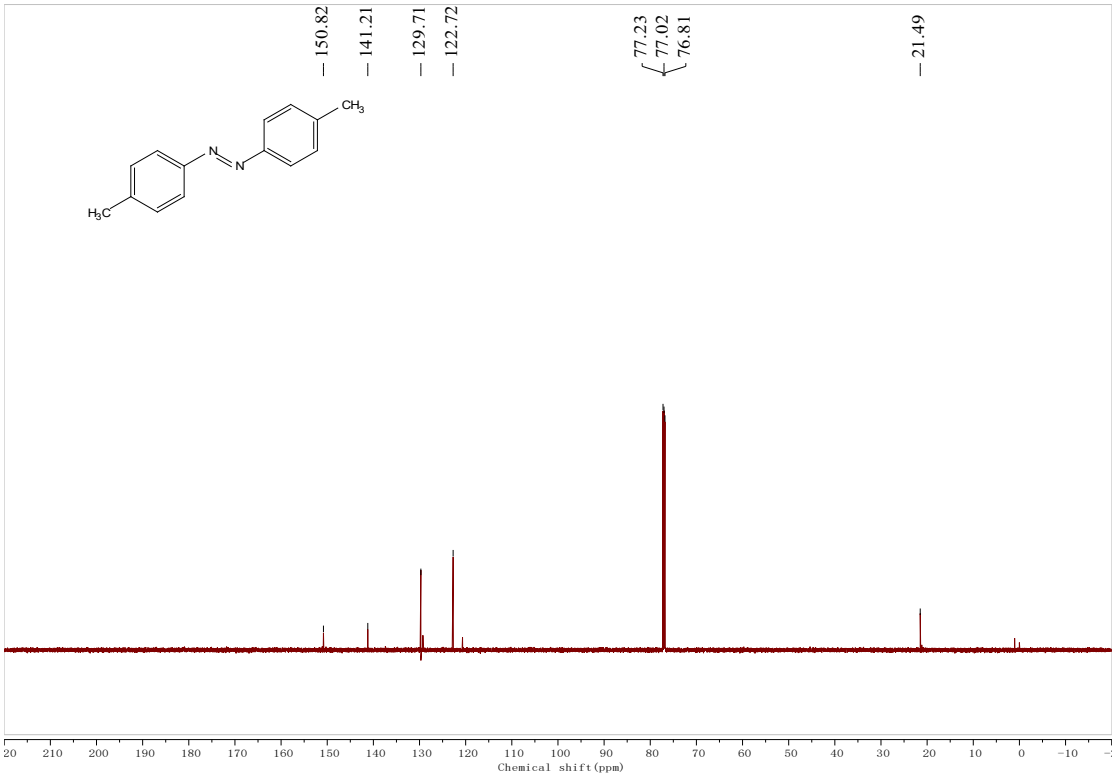


$^{13}$C NMR spectra of **6b**

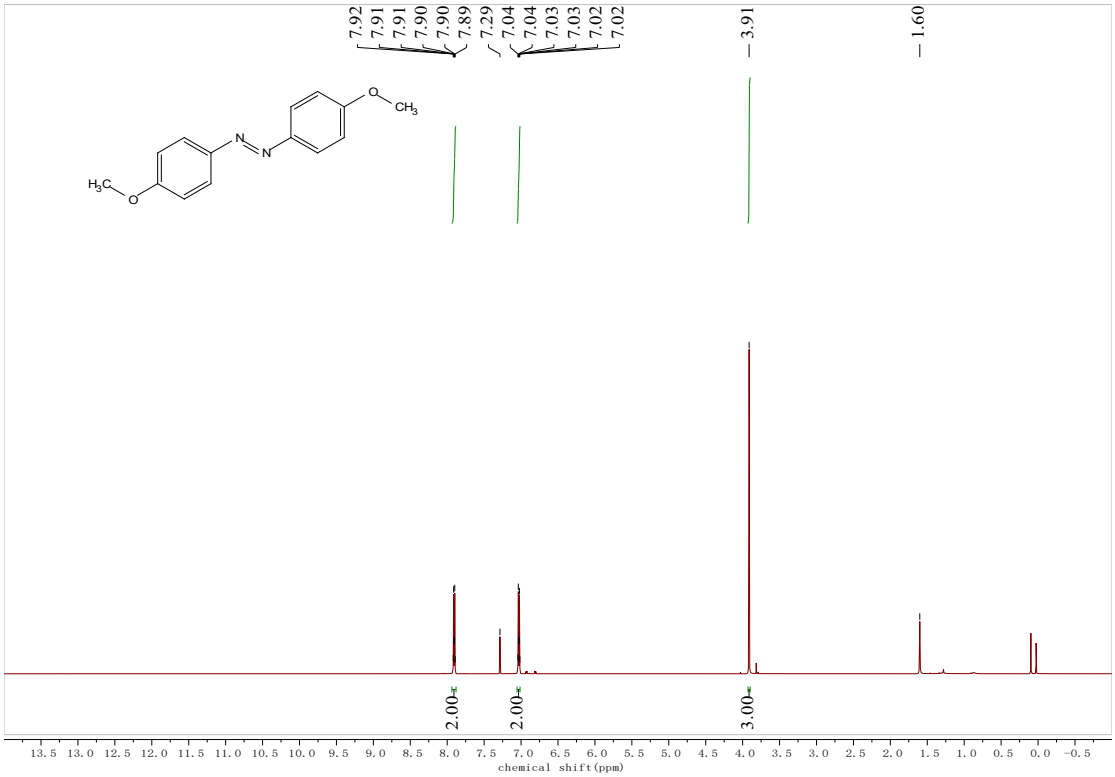


$^{1}$H NMR spectra of **6c**

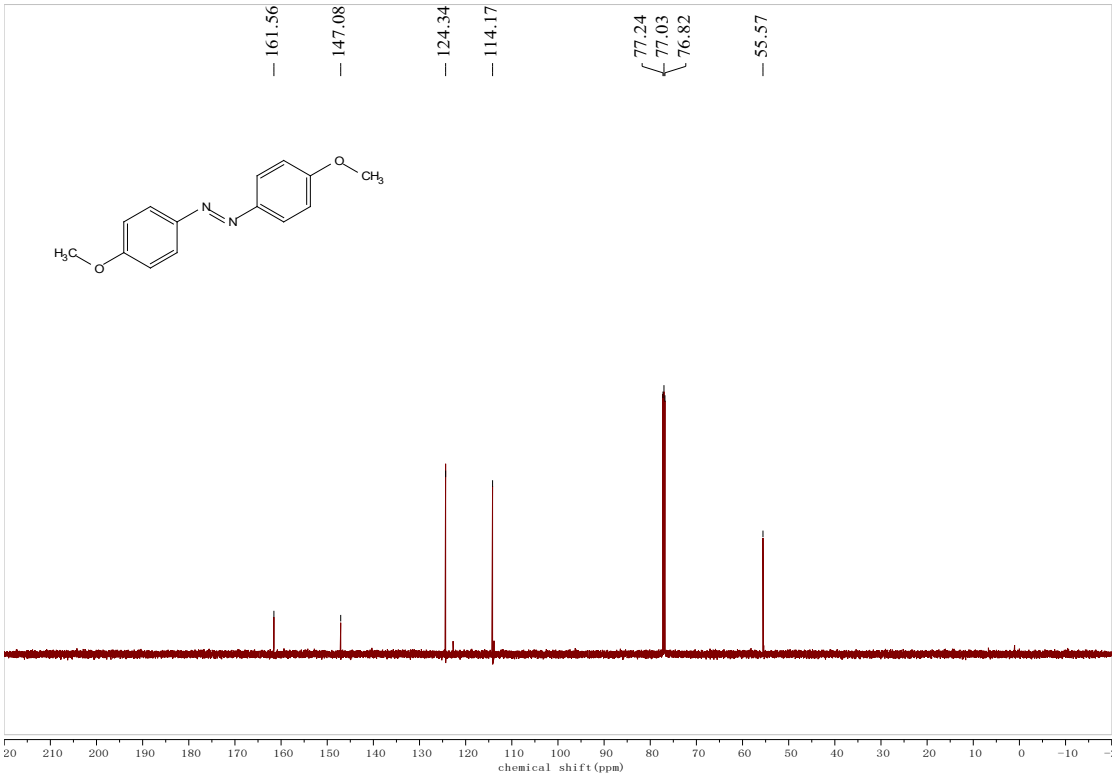


$^{13}$C NMR spectra of **6c**

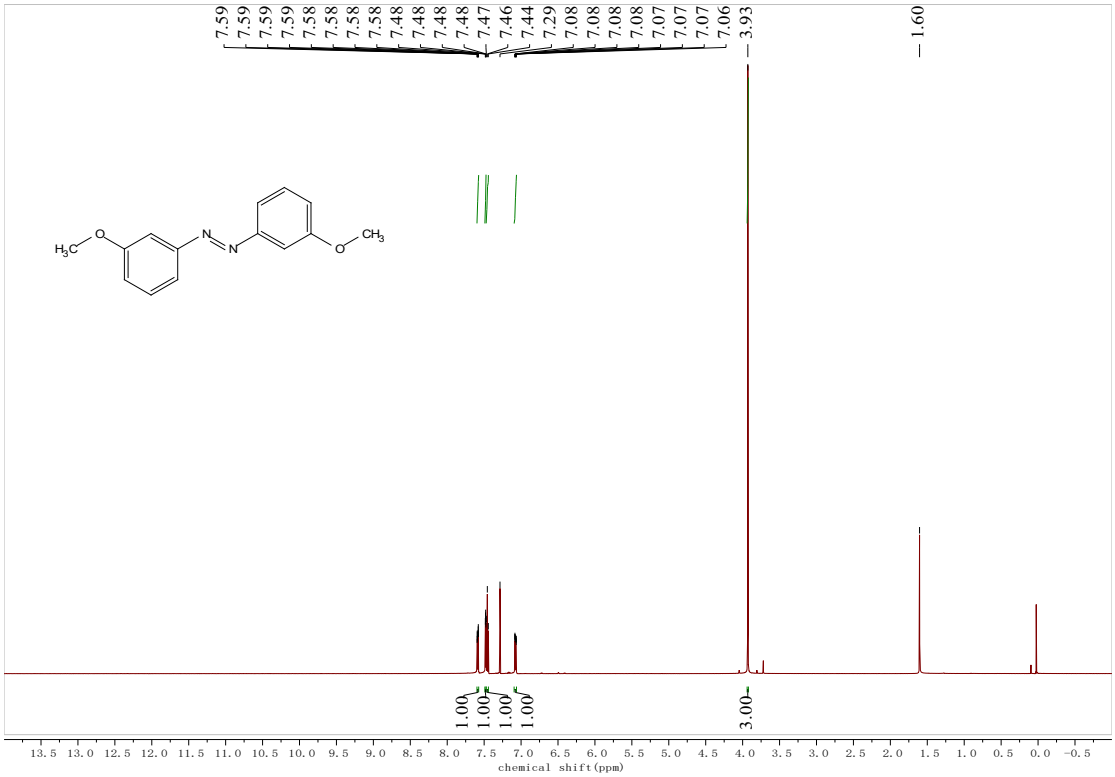


$^{1}$H NMR spectra of **6d**

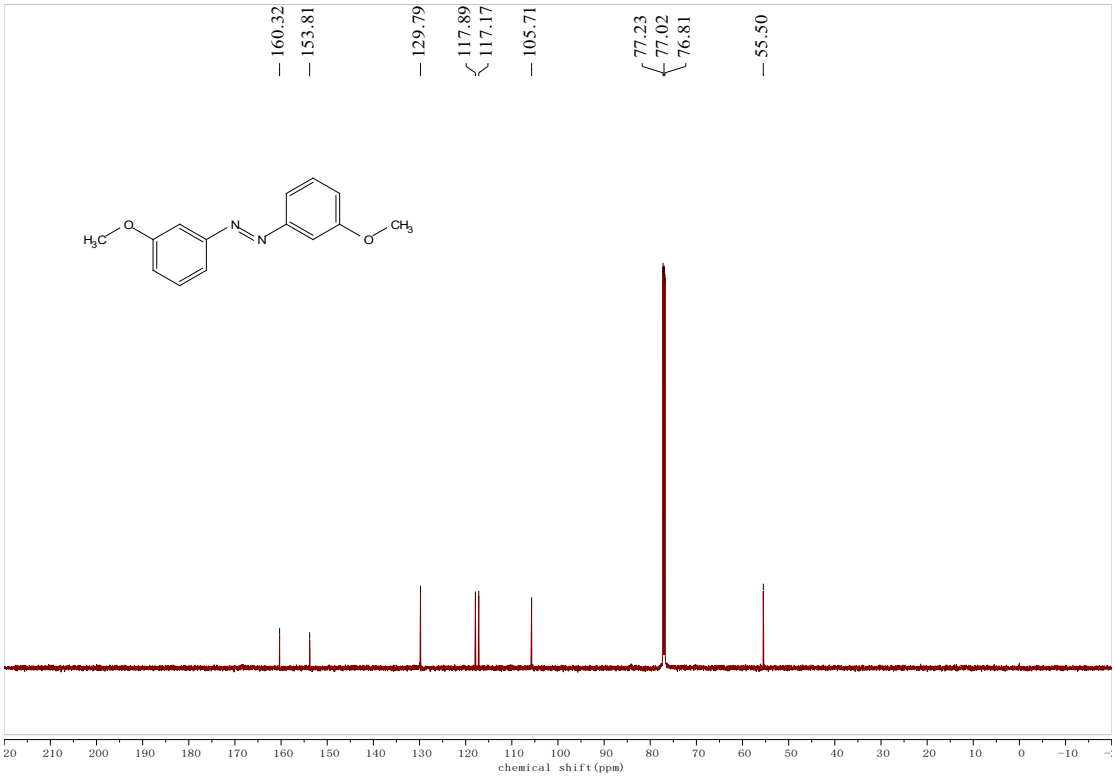


$^{13}$C NMR spectra of **6d**

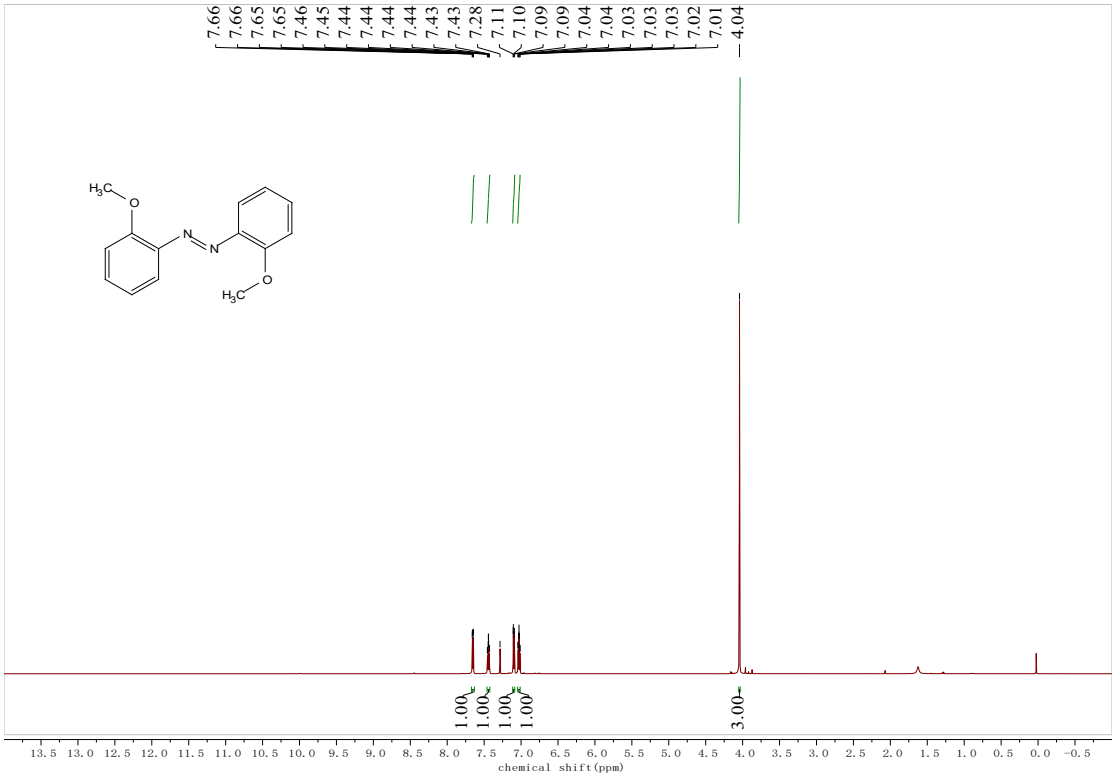


$^{1}$H NMR spectra of **6e**

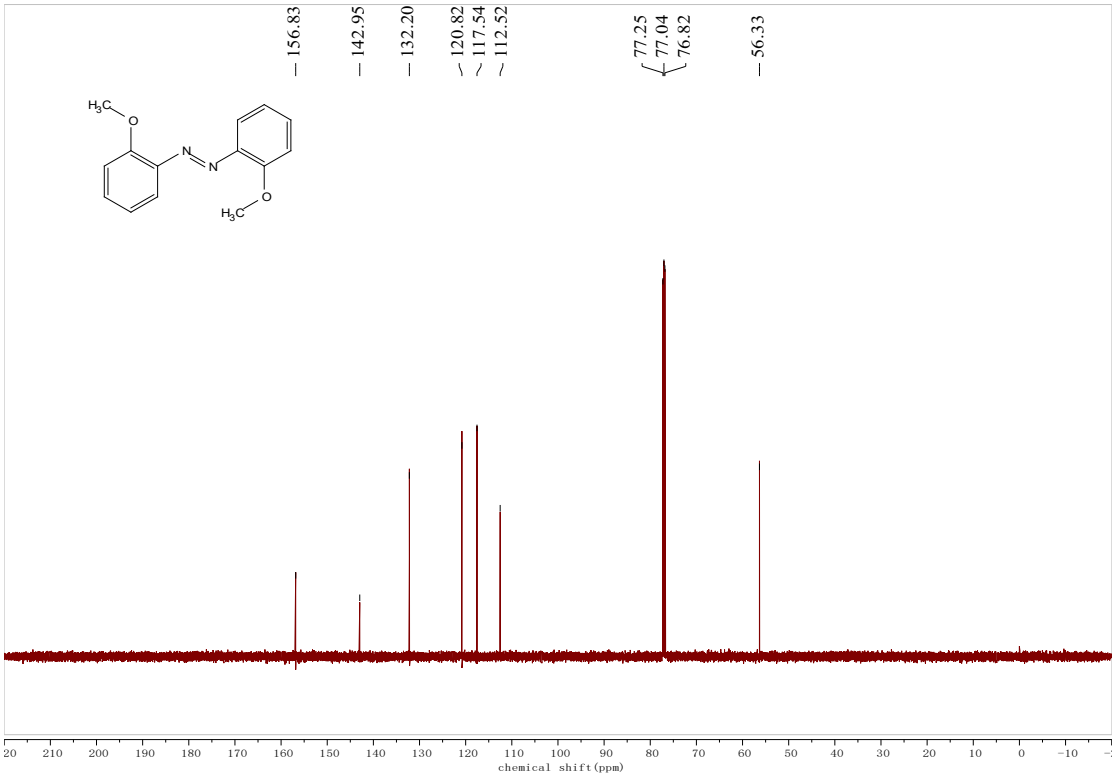


$^{13}$C NMR spectra of **6e**

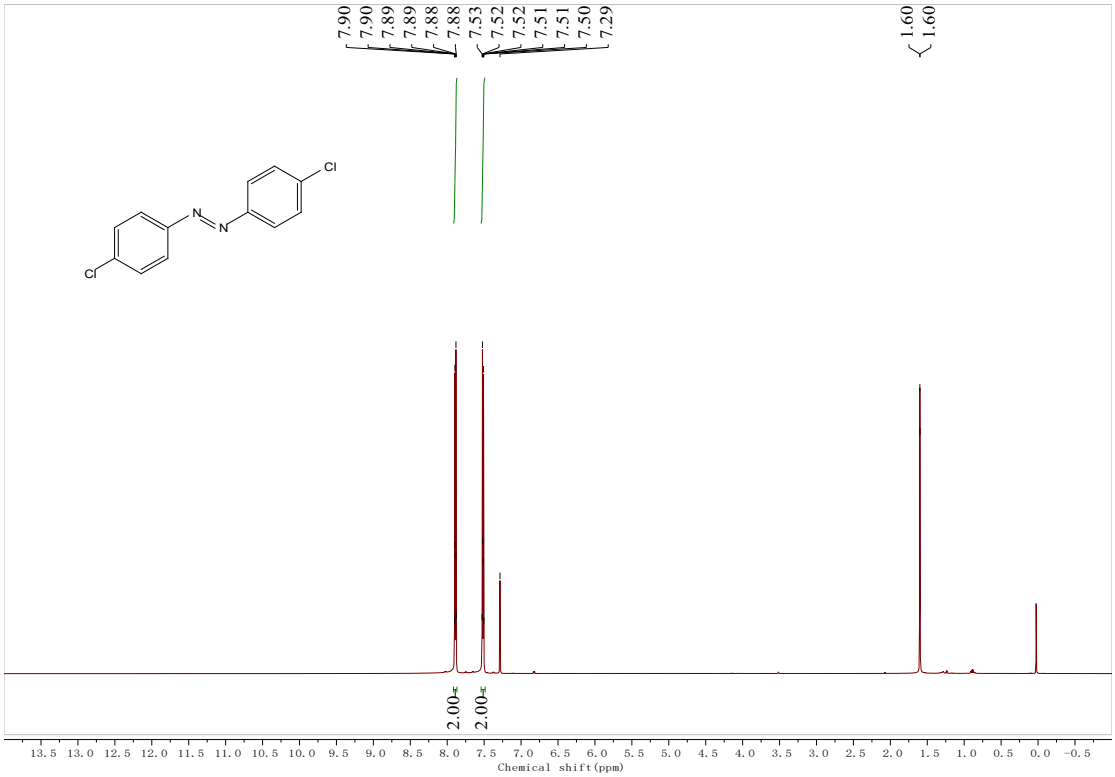


$^{1}$H NMR spectra of **6f**

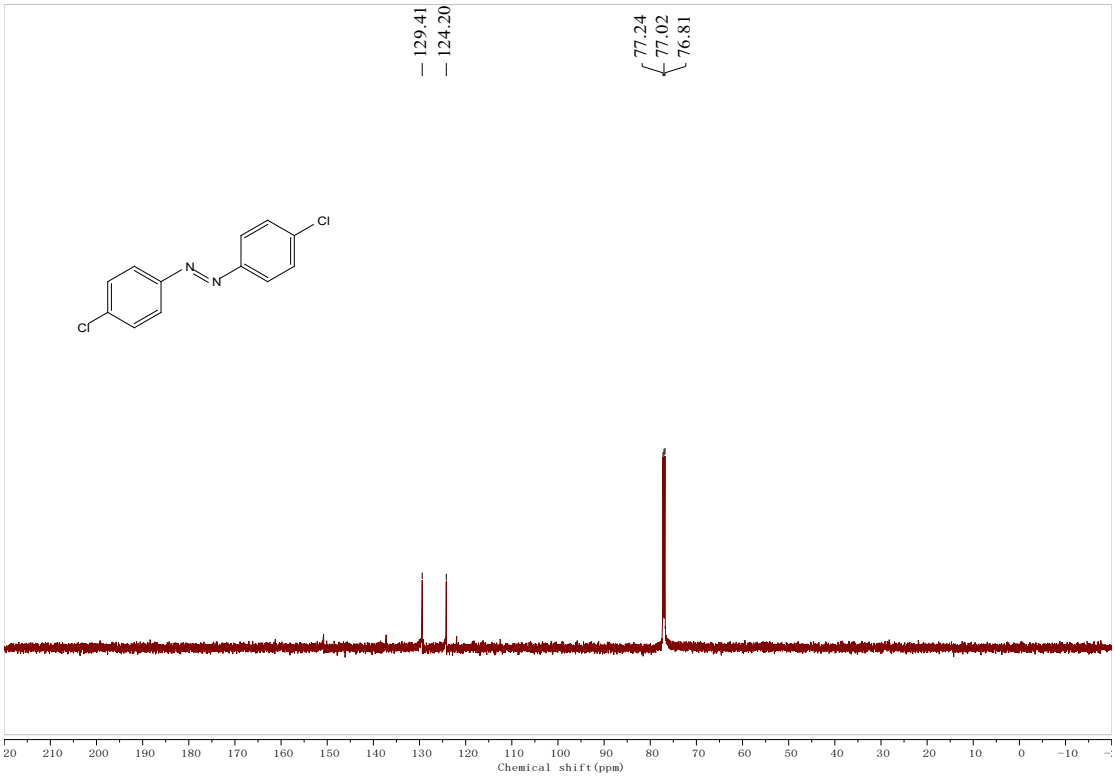


$^{13}$C NMR spectra of **6f**

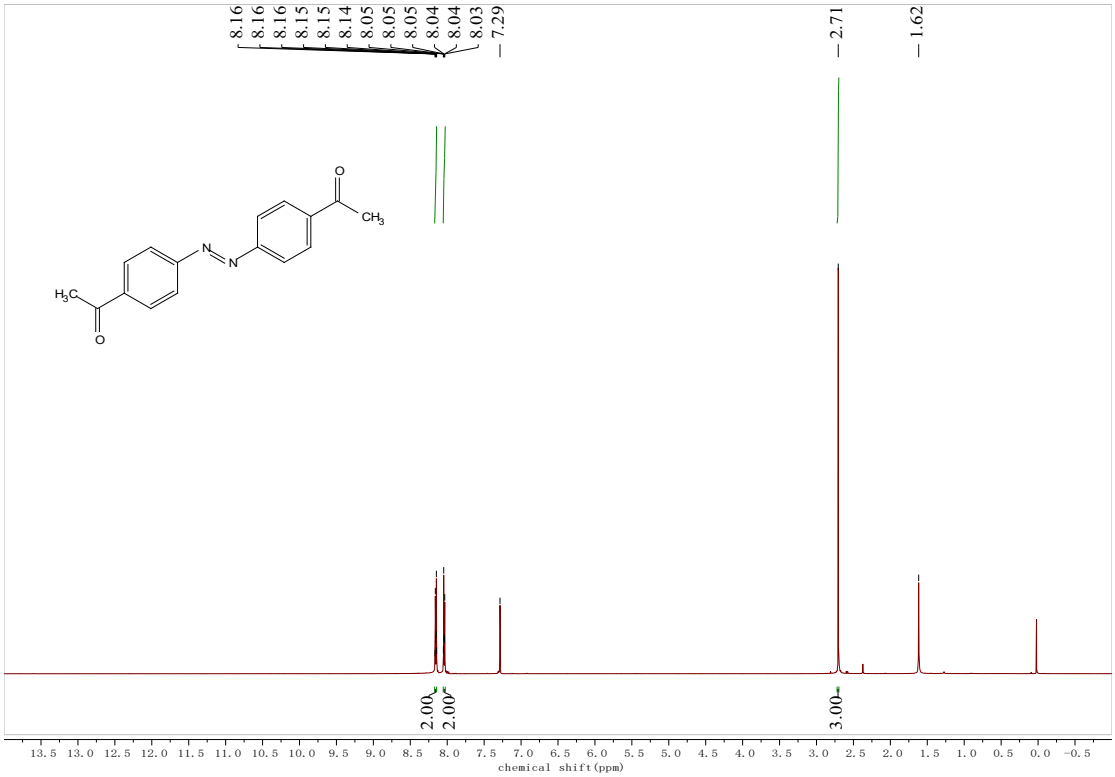


$^{1}$H NMR spectra of **6g**

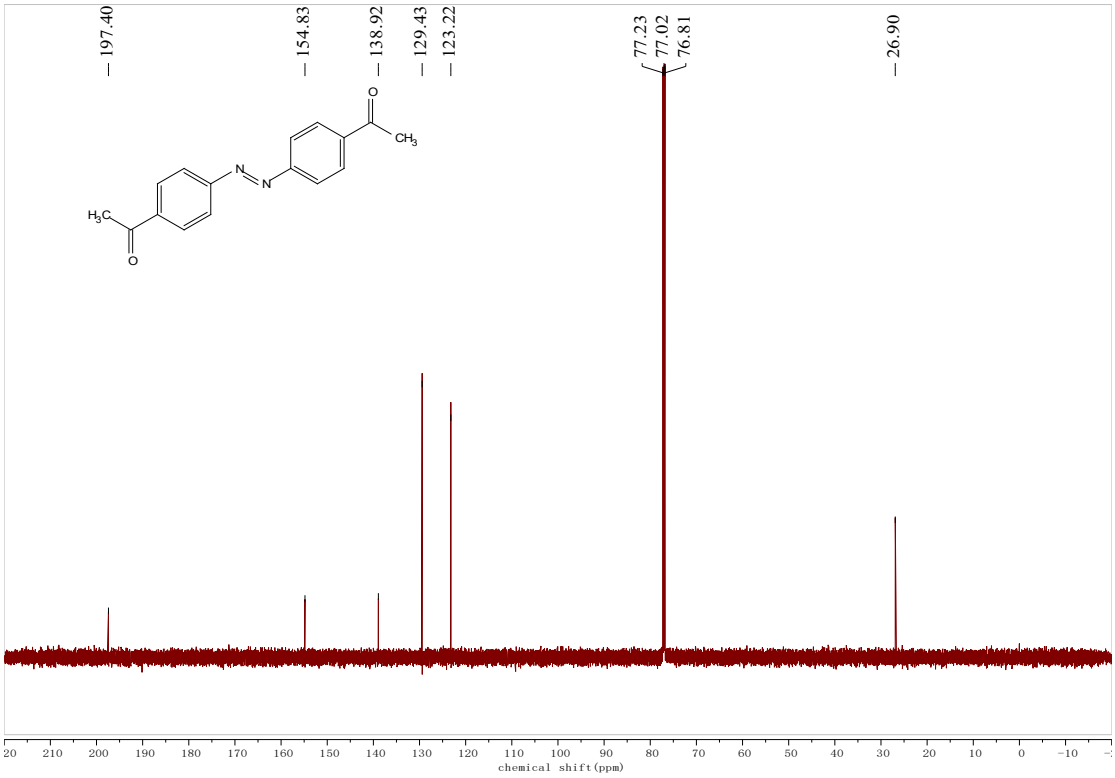


$^{13}$C NMR spectra of **6g**

## 10. Reference


1. O. V. Dolomanov, L. J. Bourhis, R. J. Gildea, J. A. K. Howard and H. Puschmann, *Journal of Applied Crystallography*, 2009, **42**, 339-341.
2. A. L. Spek, *Acta Crystallographica Section C-Structural Chemistry*, 2015, **71**, 9-18.
3. H. Shi, K. Zhang, R.-L. Lin, W.-Q. Sun, X.-F. Chu, X.-H. Liu and J.-X. Liu, *Asian J. Org. Chem.*, 2019, **8**, 339-343.
4. A. Perloff, *Inorg. Chem.*, 1970, **9**, 2228-2239.
5. C.-G. Lin, W. Chen, D.-L. Long, L. Cronin and Y.-F. Song, *Dalton Trans.*, 2014, **43**, 8587-8590.
6. H. Yu, Z. Wu, Z. Wei, Y. Zhai, S. Ru, Q. Zhao, J. Wang, S. Han and Y. Wei, *Commun. Chem.*, 2019, **2**.
7. A. Kumar, P. Sharma, N. Sharma, Y. Kumar and D. Mahajan, *RSC Adv.*, 2021, **11**, 25777-25787.
8. Z. Liu, Z. Yang, Z. Ke, X. Yu, H. Zhang, B. Yu, Y. Zhao and Z. Liu, *New J. Chem.*, 2018, **42**, 13933-13937.
9. H. Yu, Y. Zhai, G. Dai, S. Ru, S. Han and Y. Wei, *Chem. Eur. J.*, 2017, **23**, 13883-13887.
10. S. Han, Y. Cheng, S. Liu, C. Tao, A. Wang, W. Wei, H. Yu and Y. Wei, *Angew. Chem. Int. Ed.*, 2021, **60**, 6382-6385.
11. X. Liu, H. Q. Li, S. Ye, Y. M. Liu, H. Y. He and Y. Cao, *Angew. Chem. Int. Ed. Engl.*, 2014, **53**, 7624-7628.